Quantum rate equations for electron transport through an interacting system in the sequential tunneling regime

Bing Dong,[1,2] H. L. Cui,[1] and X. L. Lei[2]

[1]*Department of Physics and Engineering Physics, Stevens Institute of Technology, Hoboken, New Jersey 07030, USA*
[2]*Department of Physics, Shanghai Jiaotong University, 1954 Huashan Road, Shanghai 200030, China*
(Received 15 May 2003; revised manuscript received 20 August 2003; published 28 January 2004)

We present a set of modified quantum rate equations, with the help of the nonequilibrium Green's function and slave-particle techniques along with the correct quantization, for description of the quantum transport through an interacting mesoscopic region connected with two leads, in the sequential tunneling regime. The assumption that only leading order of $|V|^2$ (V is the tunneling coupling between the interacting central region and the leads) has been taken into account in deriving these equations implies that the quantum rate equations are only valid in the case of weak coupling between the central region and the leads. For demonstrations, we consider two special cases in the central region, a single interacting quantum dot (SQD) with weak spin-flip scattering and a weakly coupled double quantum dots (CQD), as examples. In the limit of zero temperature and large bias voltage, the resulting equations are identical to the previous results derived from the many-body Schrödinger equation. The numerical simulations reveal (1) the dependence of the spin-flip scattering on the temperature and bias voltage in the SQD, and (2) the possible negative differential conductance and negative tunnel magnetoresistance in the CQD, depending on the hopping between the two quantum dots.

I. INTRODUCTION

For many years, much experimental and theoretical work have been devoted to exploring the transport properties of artificially nanofabricated structures containing a discrete number of quantum states and a small number of electrons. The tunneling current through these mesoscopic devices, isolated from two macroscopic leads by potential barriers, manifested many novel effects due to this confinement. For example, in a semiconductor quantum dot (QD) one observed the Coulomb blockade oscillations due to the charging energy[1] and even the Kondo effect due to the strong on-site Coulomb interaction in the tunneling transport.[2,3] Recently, interest in quantum computation and quantum information processing has attracted increasing attention to the problem of measurement of tunneling currents via a mesoscopic system that can be modeled by a two-level Hamiltonian, for example, charges in coupled QD's (Refs. 4–7) and spins in a QD under magnetic fields.[8] Measurement of the tunneling current in such systems provides information not only about the Rabi oscillations[7] between the two levels but also about the spin precession in quantum spin oscillations,[9,10] both of which are crucial improvement in the control of the superposition of the quantum states and thus quantum information processing. In addition, a similar physical picture has been utilized with success to analyze transport through molecular nanojunction,[11] for example, a system of benzene[12] and DNA molecular chain.[13]

In order to describe this kind of quantum oscillations in quantum transport through a QD, the master equations or "quantum" version of the rate equations had been first proposed by Nazarov,[14] and later derived microscopically from the Schrödinger equation directly[15,16] and from the von Neumann equation and superoperators,[17] respectively. In these, the central point is that the equations of motion (EOM) of the diagonal density-matrix elements allow for an additional term of the nondiagonal density-matrix elements, which indeed stand for the coherent superposition of different quantum states and are referred to as the coherent transfer term, along with the time evolutions commanded by their own EOM. We have to solve these equations self-consistently to determine the nonequilibrium probability densities. As a result, the tunneling current unavoidably contains the contributions of the nondiagonal density-matrix elements and naturally provides the information of the quantum Rabi oscillation, although the explicit expression of current formulation only involves the diagonal density-matrix elements. The modified quantum rate equations have proved successful in describing this quantum oscillation in coherently coupled quantum dots (CQD),[14] the quantum measurement by using quantum point contact near CQD,[18–20] and even time-dependent quantum tunneling through the CQD.[21] On the other hand, the Coulomb interaction inside the small confined region plays a crucial role in, as mentioned above, determining the quantum transport properties of the devices, of course in controlling the quantum oscillations of two-level systems.[22] In fact, the so-called noninvasive quantum measurement process is also based on the Coulomb coupling between the detector and the measured system.[23,24] To our knowledge, however, a systematic investigation of the quantum rate equations at arbitrary temperature associated with the Coulomb interactions has been lacking.

About ten years ago, a "classical" rate equation was derived for sequential tunneling through a double-barrier system from the quantum kinetic equation, the nonequilibrium Green's function (NGF), which is believed to be a more powerful tool for studying nonequilibrium phenomena.[25] Our aim in this paper is to systematically explore the quantum rate equations for the interacting systems in the sequential tunneling regime from the NGF approach. The unique source of difficulty is how to deal with the Coulomb interaction

term in the derivation. This problem is the same as that we have in studies of the strongly correlated fermionic systems, for example, the recent investigations on the Kondo enhanced conductance of a QD at low temperature.[2,26,27] Many theoretical methods have been developed to solve the strong correlation effects. Among these methods, the slave-particle technique is of particular elegance.[26–28] The great advantage of this approach is that the correlated Hamiltonian for the system under study is transformed to an equivalent one without Coulomb correlations while introducing several auxiliary particles. Thus previously well-developed formulations for noninteracting systems can be applied to investigate the interacting systems in the framework of this representation. Along this line, a further technical advance is made in the present work. Here we extend the approach of the slave-particle representation to the weakly coupled quantum system of interest and give the consistent Hamiltonian formulation in terms of the slave particles. The equations of motion of the density-matrix elements are then studied in the framework of NGF and within the slave-particle scheme. Our derivation contains three approximations. The first is to assume that the central region has very "weak" coupling with the external environments (the leads) V. Second, we assume that the couplings between subsystems are also weak to keep them individual, for example, the weak spin-flip scattering in single interacting QD (SQD) and weak interdot hopping in CQD. As a result, we can give the definitions of the spectrum expressions of the NGF's of the central region in terms of the nonequilibrium probability densities and keep only the leading order term in $|V|^2$ in the expansions of the equations of motion. The final one is to apply the wide band limit in the two leads, namely, that the coupling strengths between the central region and the leads are independent of the energy and can be considered as constant.

The rest of the paper is organized as follows. In the following section, we give the derivations in detail for a SQD taking the weak spin-flip scattering into account, and establish the temperature and bias voltage dependent quantum rate equations for arbitrary Coulomb interaction. In Sec. III we derive the quantum rate equations for the weakly coupled QD's. In both the sections, after the analytical results are discussed for the no doubly occupied level and the deep level situations, we perform numerical simulations on the occupation numbers and the tunneling current in the general case as functions of the bare level in the QD and the bias voltage between the source and the drain. Finally, all the results are summarized in Sec. V.

II. SINGLE QUANTUM DOT

We begin with our derivation of the quantum rate equations for a SQD with a weak spin-flip scattering in this section. In the case of no spin-flip terms, the rate equations are of classical variety, which have been adequately described by other methods. Therefore our results are not new in this case but are established from a different scheme. The purpose of this section is also to provide an examination to prove this approach in comparison with the previous results in no spin-flip case.
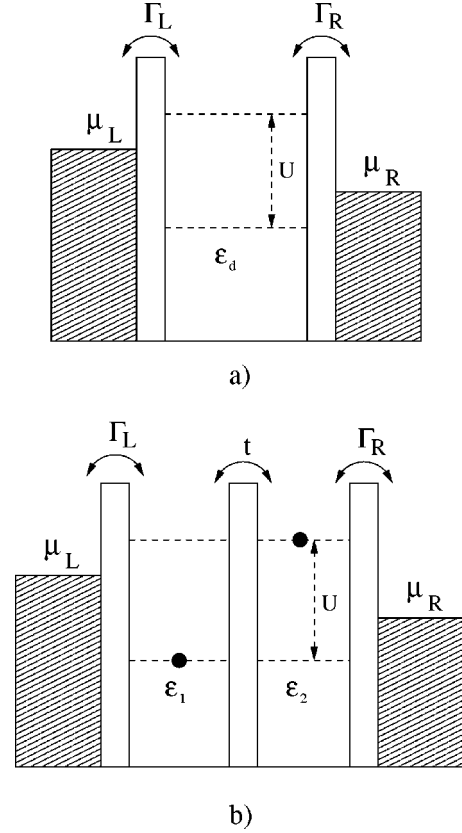

FIG. 1. Schematic diagrams for the resonant tunneling through (a) a single interacting QD and (b) a coherently coupled QD's.

A. Model Hamiltonian and slave-particle representation

We use the standard model Hamiltonian to describe the resonant tunneling through a SQD, as depicted in Fig. 1(a), with a single bare level ϵ_d and a weak intradot spin-flip scattering R_σ connected to two noninteracting leads:

$$H = \sum_{\eta,k,\sigma} \epsilon_{\eta k\sigma} c^\dagger_{\eta k\sigma} c_{\eta k\sigma} + \epsilon_d \sum_\sigma c^\dagger_{d\sigma} c_{d\sigma} + R_\uparrow c^\dagger_{d\uparrow} c_{d\downarrow}$$

$$+ R_\downarrow c^\dagger_{d\downarrow} c_{d\uparrow} + U n_{d\uparrow} n_{d\downarrow} + \sum_{\eta,k,\sigma} (V_{\eta\sigma} c^\dagger_{\eta k\sigma} c_{d\sigma} + \text{H.c.}),$$

$$(1)$$

where $c^\dagger_{\eta k\sigma}$ ($c_{\eta k\sigma}$) and $c^\dagger_{d\sigma}$ ($c_{d\sigma}$) are the creation (annihilation) operators for electrons with momentum k, spin σ, and energy $\epsilon_{\eta k\sigma}$ in the lead η ($=L,R$) and for a spin-σ electron on the QD, respectively. The third term describes the Coulomb interaction among electrons on the QD. $n_{d\sigma} = c^\dagger_{d\sigma} c_{d\sigma}$ is the occupation operator in the SQD. The fourth term represents the tunneling coupling between the QD and the reservoirs. We assume that the coupling strength $V_{\eta\sigma}$ is spin dependent, being able to describe the ferromagnetic leads. Each of the two leads is separately in thermal equilibrium with the chemical potential μ_η, which is assumed to be zero in equilibrium condition and chosen as the energy reference throughout the paper. In the nonequilibrium case, the chemical potentials of the leads differ by the applied bias. In this

paper, we assume that the tunneling coupling is weak enough to guarantee no Kondo effect in our model and the QD is in the Coulomb blockade regime. Generally, we have $R_\uparrow = R_\downarrow^* = R$ as a constant.

According to the finite-U slave-boson approach introduced by Zou and Anderson,[29] the electron operator $c_{d\sigma}$ can be written in four possible single-electron states, namely, the empty state $|0\rangle$ with zero energy $\varepsilon_0 = 0$, the singly occupied (with spin up or down) electronic state $|\sigma\rangle$ with energy $\varepsilon_\sigma = \epsilon_d$, and the doubly occupied state $|\uparrow\downarrow\rangle$ with energy $\varepsilon_d = 2\epsilon_d + U$, as

$$c_{d\sigma} = |0\rangle\langle\sigma| + \sigma|\bar{\sigma}\rangle\langle\uparrow\downarrow| \quad (\sigma = \pm 1). \tag{2}$$

Because these four states expand the entire Hilbert space, the completeness relation must be satisfied

$$|0\rangle\langle 0| + |\uparrow\downarrow\rangle\langle\uparrow\downarrow| + \sum_\sigma |\sigma\rangle\langle\sigma| = 1. \tag{3}$$

These Dirac brackets were then treated as operators: $e^\dagger = |0\rangle$, $d^\dagger = |\uparrow\downarrow\rangle$ as slave-boson operators and $f_\sigma^\dagger = |\sigma\rangle$ as pseudofermion operator. In terms of these auxiliary operators, Eqs. (2) and (3) become

$$c_{d\sigma} = e^\dagger f_\sigma + \sigma f_{\bar{\sigma}}^\dagger d, \tag{4}$$

$$e^\dagger e + d^\dagger d + \sum_\sigma f_\sigma^\dagger f_\sigma = 1. \tag{5}$$

The explicit (anti)communicators of these auxiliary particles can be easily established from the definitions of the Dirac brackets:[30]

$$ee^\dagger = 1, \quad dd^\dagger = 1, \quad f_\sigma f_{\sigma'}^\dagger = \delta_{\sigma\sigma'},$$

$$ed^\dagger = ef_\sigma^\dagger = f_\sigma e^\dagger = f_\sigma d^\dagger = de^\dagger = df_\sigma^\dagger = 0. \tag{6}$$

Therefore, along with these correct quantization, the Hamiltonian (1) can be replaced by the following form in the auxiliary particle representation:

$$H = \sum_{\eta,k,\sigma} \epsilon_{\eta k\sigma} c_{\eta k\sigma}^\dagger c_{\eta k\sigma} + \epsilon_d \sum_\sigma f_\sigma^\dagger f_\sigma + (2\epsilon_d + U)d^\dagger d$$

$$+ R_\uparrow f_\uparrow^\dagger f_\downarrow + R_\downarrow f_\downarrow^\dagger f_\uparrow + \sum_{\eta,k,\sigma} [V_{\eta\sigma} c_{\eta k\sigma}^\dagger (e^\dagger f_\sigma + \sigma f_{\bar{\sigma}}^\dagger d)$$

$$+ \text{H.c.}], \tag{7}$$

which was proved to be equivalent to the original one, Eq. (1), by Zou and Anderson in the case of no spin-flip term.[29]

Furthermore, as far as the four possible single electric states are considered as the basis, the statistical expectations of the diagonal elements of the density-matrix, ρ_{ii} ($i = \{0,\sigma,d\}$), give the occupation probabilities of the resonant level in the QD being empty, or singly occupied by spin-σ electron, or doubly occupied, respectively. The nondiagonal term $\rho_{\uparrow\downarrow}$ describes the coherent superposition state between the spin-up and -down states in the QD. In the slave-particle notation, the corresponding relations between the density-

matrix elements and these auxiliary operators are obvious as $\hat{\rho}_{00} = |0\rangle\langle 0| = e^\dagger e$, $\hat{\rho}_{\sigma\sigma} = |\sigma\rangle\langle\sigma| = f_\sigma^\dagger f_\sigma$, $\hat{\rho}_{dd} = |\uparrow\downarrow\rangle\langle\uparrow\downarrow| = d^\dagger d$, and the nondiagonal term $\hat{\rho}_{\sigma\bar{\sigma}} = |\bar{\sigma}\rangle\langle\sigma| = f_{\bar{\sigma}}^\dagger f_\sigma$. According to Eq. (5), the constraint is subject to the diagonal elements of the density-matrix $\hat{\rho}_{00} + \Sigma_\sigma\hat{\rho}_{\sigma\sigma} + \hat{\rho}_{dd} = 1$.

B. Derivation of the quantum rate equations

In this section, we derive the rate equations for sequential tunneling starting from the combined fermion-boson Hamiltonian (7) by using the Keldysh's NGF.

In order to describe the nonequilibrium state of electrons, we define the retarded (advanced) and lesser (greater) Green's functions (GFs) for the QD $G_{\sigma\sigma'}^{r(a),<(>)}(t,t') \equiv \langle\langle c_{d\sigma}(t)|c_{d\sigma'}^\dagger(t')\rangle\rangle^{r(a),<(>)}$ as follows: $G_{\sigma\sigma'}^{r(a)}(t,t') \equiv \pm i\theta(\pm t\mp t')\langle\{c_{d\sigma}(t),c_{d\sigma'}^\dagger(t')\}\rangle$, $G_{\sigma\sigma'}^<(t,t') \equiv i\langle c_{d\sigma'}^\dagger(t')c_{d\sigma}(t)\rangle$, and $G_{\sigma\sigma'}^>(t,t') \equiv -i\langle c_{d\sigma}(t)c_{d\sigma'}^\dagger(t')\rangle$. Considering Eq. (4), these GF's in the QD can be divided into two parts, $G_{\sigma\sigma'} = G_{e\sigma\sigma'} + G_{d\bar{\sigma}\bar{\sigma}'}$ with $G_{e\sigma\sigma'} \equiv \langle\langle e^\dagger(t)f_\sigma(t)|f_{\sigma'}^\dagger(t')e(t')\rangle\rangle$ and $G_{d\bar{\sigma}\bar{\sigma}'} = \sigma\sigma'\langle\langle f_{\bar{\sigma}}^\dagger(t)d(t)|d^\dagger(t')f_{\bar{\sigma}'}(t')\rangle\rangle$. Under the weak-coupling assumption, the central region can be regarded as a considerably isolated system and its density-matrix operator is supposed to be $\hat{\rho} = \Sigma_{ij}\rho_{ij}\hat{\rho}_{ij}$ ($i,j = \{0,\sigma,d\}$), meanwhile the reservoirs are taken as "environment" located in local thermal equilibrium. Therefore, we can readily define the decoupled diagonal GF's of the QD for weak spin-flip transitions in terms of spectrum expression, in the Fourier space, as

$$G_{e\sigma\sigma}^{r0}(\omega) = \frac{\rho_{00} + \rho_{\sigma\sigma}}{\omega - \epsilon_d + i0^+},$$

$$G_{d\bar{\sigma}\bar{\sigma}}^{r0}(\omega) = \frac{\rho_{dd} + \rho_{\bar{\sigma}\bar{\sigma}}}{\omega - (\epsilon_d + U) + i0^+},$$

$$G_{e\sigma\sigma}^{<0}(\omega) = 2\pi i\rho_{\sigma\sigma}\delta(\omega - \epsilon_d),$$

$$G_{d\bar{\sigma}\bar{\sigma}}^{<0}(\omega) = 2\pi i\rho_{dd}\delta[\omega - (\epsilon_d + U)],$$

$$G_{e\sigma\sigma}^{>0}(\omega) = -2\pi i\rho_{00}\delta(\omega - \epsilon_d),$$

$$G_{d\bar{\sigma}\bar{\sigma}}^{>0}(\omega) = -2\pi i\rho_{\bar{\sigma}\bar{\sigma}}\delta[\omega - (\epsilon_d + U)]. \tag{8}$$

If no bias voltage is added between the two leads, the central region is in a thermal equilibrium state and the distribution probabilities are well known as $\rho_{00} = 1/Z$, $\rho_{\sigma\sigma} = e^{-\epsilon_d/T}/Z$, and $\rho_{dd} = e^{-(2\epsilon_d + U)/T}/Z$ with $Z = 1 + 2e^{-\epsilon_d/T} + e^{-(2\epsilon_d + U)/T}$. As far as the spin-flip transition is considered, the decoupled nondiagonal correlation GFs are crucial in the following derivation. Their Fourier expressions are easily obtained from the definitions as

$$G_{e\sigma\bar{\sigma}}^{<0}(\omega) = 2\pi i\rho_{\sigma\bar{\sigma}}\delta(\omega - \epsilon_d),$$

$$G_{d\bar{\sigma}\sigma}^{>0}(\omega) = 2\pi i\rho_{\sigma\bar{\sigma}}\delta[\omega - (\epsilon_d + U)],$$

$$G_{d\sigma\bar{\sigma}}^{<0}(\omega) = 0, \quad G_{e\sigma\bar{\sigma}}^{>0}(\omega) = 0. \tag{9}$$

For the case of nonequilibrium discussed here, these out-of-equilibrium probabilities are determined by the coupling to environments with different chemical potentials, and usually they obey a set of equations of time evolution, the rate equations.

Here, we start from the equations of motion of the operators $\hat{\rho}_{ij}$ with the Hamiltonian (7) and modified quantization Eq. (6):

$$\dot{\hat{\rho}}_{00}=i[H,e^{\dagger}e]=-i\sum_{\eta,k,\sigma}(V_{\eta\sigma}c^{\dagger}_{\eta k\sigma}e^{\dagger}f_{\sigma}-V^{*}_{\eta\sigma}f^{\dagger}_{\sigma}ec_{\eta k\sigma}),$$
(10a)

$$\dot{\hat{\rho}}_{\sigma\sigma}=i[H,f^{\dagger}_{\sigma}f_{\sigma}]=i\sum_{\eta,k}(V_{\eta\sigma}c^{\dagger}_{\eta k\sigma}e^{\dagger}f_{\sigma}-\bar{\sigma}V_{\eta\bar{\sigma}}c^{\dagger}_{\eta k\bar{\sigma}}f^{\dagger}_{\sigma}d$$
$$-V^{*}_{\eta\sigma}f^{\dagger}_{\sigma}ec_{\eta k\sigma}+\bar{\sigma}V^{*}_{\eta\bar{\sigma}}d^{\dagger}f_{\sigma}c_{\eta k\bar{\sigma}})$$
$$+iR_{\bar{\sigma}}f^{\dagger}_{\bar{\sigma}}f_{\sigma}-iR_{\sigma}f^{\dagger}_{\sigma}f_{\bar{\sigma}},$$
(10b)

$$\dot{\hat{\rho}}_{\bar{\sigma}\bar{\sigma}}=i[H,f^{\dagger}_{\bar{\sigma}}f_{\sigma}]=i\sum_{\eta,k}(V_{\eta\bar{\sigma}}c^{\dagger}_{\eta k\bar{\sigma}}e^{\dagger}f_{\sigma}-\bar{\sigma}V_{\eta\sigma}c^{\dagger}_{\eta k\sigma}f^{\dagger}_{\bar{\sigma}}d$$
$$-V^{*}_{\eta\sigma}f^{\dagger}_{\bar{\sigma}}ec_{\eta k\sigma}+\sigma V^{*}_{\eta\sigma}d^{\dagger}f_{\sigma}c_{\eta k\sigma})$$
$$+iR_{\sigma}(f^{\dagger}_{\sigma}f_{\sigma}-f^{\dagger}_{\bar{\sigma}}f_{\bar{\sigma}}),$$
(10c)

$$\dot{\hat{\rho}}_{dd}=i[H,d^{\dagger}d]=i\sum_{\eta,k,\sigma}\sigma(V_{\eta\sigma}c^{\dagger}_{\eta k\sigma}f^{\dagger}_{\bar{\sigma}}d-V^{*}_{\eta\sigma}d^{\dagger}f_{\bar{\sigma}}c_{\eta k\sigma}).$$
(10d)

Their statistical expectations involve the time-diagonal parts of the correlation functions:

$$G^{<}_{e\sigma,\eta k\sigma'}(t,t')\equiv i\langle c^{\dagger}_{\eta k\sigma'}(t')e^{\dagger}(t)f_{\sigma}(t)\rangle,$$

$$G^{<}_{d\sigma',\eta k\sigma}(t,t')\equiv i\langle c^{\dagger}_{\eta k\sigma}(t')f^{\dagger}_{\sigma'}(t)d(t)\rangle,$$

$$G^{<}_{\eta k\sigma',e\sigma}(t,t')\equiv i\langle f^{\dagger}_{\sigma}(t')e(t')c_{\eta k\sigma'}(t)\rangle,$$

and

$$G^{<}_{\eta k\sigma,d\sigma'}(t,t')\equiv i\langle d^{\dagger}(t')f_{\sigma'}(t')c_{\eta k\sigma}(t)\rangle.$$

With the help of the Langreth analytic continuation rules,[31] we obtain the following expressions in the wide band limit (the detail derivation will be given in the Appendix):

$$\dot{\rho}_{00}=-\frac{i}{2\pi}\int d\omega\sum_{\eta,\sigma}\{\Gamma_{\eta\sigma}f_{\eta}(\omega)G^{>}_{e\sigma\sigma}(\omega)$$
$$+\Gamma_{\eta\sigma}[1-f_{\eta}(\omega)]G^{<}_{e\sigma\sigma}(\omega)\},$$
(11a)

$$\dot{\rho}_{\sigma\sigma}=\frac{i}{2\pi}\int d\omega\sum_{\eta}\{\Gamma_{\eta\sigma}f_{\eta}(\omega)G^{>}_{e\sigma\sigma}(\omega)$$
$$+\Gamma_{\eta\sigma}[1-f_{\eta}(\omega)]G^{<}_{e\sigma\sigma}(\omega)-\Gamma_{\eta\bar{\sigma}}f_{\eta}(\omega)G^{>}_{d\sigma\sigma}(\omega)$$
$$-\Gamma_{\eta\bar{\sigma}}[1-f_{\eta}(\omega)]G^{<}_{d\sigma\sigma}(\omega)\}+iR_{\bar{\sigma}}\rho_{\sigma\bar{\sigma}}-iR_{\sigma}\rho_{\bar{\sigma}\sigma},$$
(11b)

$$\dot{\rho}_{\sigma\bar{\sigma}}=\frac{i}{4\pi}\int d\omega\sum_{\eta}(\Gamma_{\eta\sigma}+\Gamma_{\eta\bar{\sigma}})\{f_{\eta}(\omega)G^{>}_{e\sigma\bar{\sigma}}(\omega)$$
$$+[1-f_{\eta}(\omega)]G^{<}_{e\sigma\bar{\sigma}}(\omega)-f_{\eta}(\omega)G^{>}_{d\sigma\bar{\sigma}}(\omega)$$
$$-[1-f_{\eta}(\omega)]G^{<}_{d\sigma\bar{\sigma}}(\omega)\}+iR_{\sigma}(\rho_{\sigma\sigma}-\rho_{\bar{\sigma}\bar{\sigma}}),$$
(11c)

$$\dot{\rho}_{dd}=\frac{i}{2\pi}\int d\omega\sum_{\eta,\sigma}\{\Gamma_{\eta\sigma}f_{\eta}(\omega)G^{>}_{d\sigma\bar{\sigma}}(\omega)$$
$$+\Gamma_{\eta\sigma}[1-f_{\eta}(\omega)]G^{<}_{d\sigma\bar{\sigma}}(\omega)\}$$
(11d)

in terms of the QD's GFs in the Fourier space.[32] Here $\Gamma_{\eta\sigma}=2\pi\Sigma_{k}|V_{\eta\sigma}|^{2}\delta(\omega-\epsilon_{\eta k\sigma})$ denotes the strength of coupling between the QD level and the lead η. In wide band limit, it is independent of energy and is supposed to be constant. Under the weak-coupling assumption, it is adequate to keep only the leading order of $|V|^{2}$ in evaluation of these occupation densities. So we can replace these QD's GFs with their decoupled formulas, Eqs. (8) and (9). Finally, the resulting quantum rate equations become

$$\dot{\rho}_{00}=\sum_{\sigma}(\Gamma^{-}_{\sigma}\rho_{\sigma\sigma}-\Gamma^{+}_{\sigma}\rho_{00}),$$
(12a)

$$\dot{\rho}_{\sigma\sigma}=\Gamma^{+}_{\sigma}\rho_{00}+\tilde{\Gamma}^{-}_{\bar{\sigma}}\rho_{dd}-(\Gamma^{-}_{\sigma}+\tilde{\Gamma}^{+}_{\bar{\sigma}})\rho_{\sigma\sigma}-2\text{Im}(R_{\bar{\sigma}}\rho_{\sigma\bar{\sigma}}),$$
(12b)

$$\dot{\rho}_{\sigma\bar{\sigma}}=iR_{\sigma}(\rho_{\sigma\sigma}-\rho_{\bar{\sigma}\bar{\sigma}})-\tfrac{1}{2}(\tilde{\Gamma}^{+}_{\sigma}+\tilde{\Gamma}^{+}_{\bar{\sigma}}+\Gamma^{-}_{\sigma}+\Gamma^{-}_{\bar{\sigma}})\rho_{\sigma\bar{\sigma}},$$
(12c)

$$\dot{\rho}_{dd}=\tilde{\Gamma}^{+}_{\downarrow}\rho_{\uparrow\uparrow}+\tilde{\Gamma}^{+}_{\uparrow}\rho_{\downarrow\downarrow}-(\tilde{\Gamma}^{-}_{\uparrow}+\tilde{\Gamma}^{-}_{\downarrow})\rho_{dd},$$
(12d)

together with the normalization relation $\rho_{00}+\rho_{dd}+\Sigma_{\sigma}\rho_{\sigma\sigma}=1$ from Eq. (3), with the definitions $\Gamma^{\pm}_{\sigma}=\Sigma_{\eta}\Gamma_{\eta\sigma}f^{\pm}_{\eta}(\epsilon_{d})$ and $\tilde{\Gamma}^{\pm}_{\sigma}=\Sigma_{\eta}\Gamma_{\eta\sigma}f^{\pm}_{\eta}(\epsilon_{d}+U)$, where $f^{+}_{\eta}(\omega)=\{1+e^{(\omega-\mu_{\eta})/T}\}^{-1}$ is the Fermi distribution function of the η lead and $f^{-}(\omega)=1-f^{+}(\omega)$. Here, Γ^{+}_{σ} (Γ^{-}_{σ}) describes the tunneling rate of electrons with spin σ into (out from) the QD without the occupation of the $\bar{\sigma}$ state. Similarly, $\tilde{\Gamma}^{+}_{\sigma}$ ($\tilde{\Gamma}^{-}_{\sigma}$) describes the tunneling rate of electrons with spin σ into (out from) the QD, when the QD is already occupied by an electron with spin $\bar{\sigma}$, revealing the modification of the corresponding rates due to the Coulomb repulsion.

These rate equations, Eqs. (12a), (12b), and (12d) coincide with the previous classical rate equations in the sequential picture for the resonant tunneling if the intradot spin-flip transition is quenched.[33,34] Obviously, if the left lead has the same chemical potential as the right lead, the stationary solutions of Eqs. (12a), (12b), and (12d) reduce exactly to the above-mentioned thermal equilibrium results in the case of $R=0$. In this situation, they have clear classical interpretations. For example, the rate of change of the number of the spin-σ electrons $\rho_{\sigma\sigma}$ in the SQD, described by Eq. (12b), is contributed from the following four single-particle tunneling processes: (1) tunneling into the QD with spin-σ electrons Γ^{+}_{σ} from both left and right leads if the QD is initially in the empty state ρ_{00}; (2) tunneling out from the QD with spin-$\bar{\sigma}$

electrons $\tilde{\Gamma}_{\bar{\sigma}}^-$ into both two leads if the QD is initially in the doubly occupied state ρ_{dd}; (3) tunneling into the QD with spin-$\bar{\sigma}$ electrons $\tilde{\Gamma}_{\bar{\sigma}}^+$ from both two leads; and (4) tunneling out from the QD with spin-σ electrons $\Gamma_{\bar{\sigma}}^-$ into both two leads, when the QD is initially just in the state $\rho_{\sigma\sigma}$. Tunneling events (1) and (2) increase the probability of the spin-σ state, but events (3) and (4) decrease this probability. These contributions constitute the classical rate equation form. Other diagonal equations have similar interpretations. Notice that the final term in Eq. (12b) describes transitions between isolated states through the coupling with nondiagonal terms, which has no classical counterpart. Therefore, it is responsible for coherent effects in the transport.

The nondiagonal matrix element $\rho_{\sigma\bar{\sigma}}$ is ruled by Eq. (12c), which resembles the optical Bloch equation and describes the dynamics of quantum superposition. This is a pure quantum effect. As mentioned by Gurvitz and Prager,[15] the couplings with the leads (all possible tunneling processes involved) always provide negative contribution and cause damping of the quantum superposition.

The particle current I_η flowing from the lead η to the QD can be evaluated from the rate of time change of the electron number operator $N_\eta(t)=\Sigma_{k,\sigma}c_{\eta k\sigma}^\dagger(t)c_{\eta k\sigma}(t)$ of the lead η:[32]

$$
\begin{aligned}
I_\eta(t) &= -\frac{e}{\hbar}\left\langle\frac{dN_\eta}{dt}\right\rangle \\
&= -i\frac{e}{\hbar}\left\langle\left[H,\sum_{k,\sigma}c_{\eta k\sigma}^\dagger(t)c_{\eta k\sigma}(t)\right]\right\rangle \\
&= i\frac{e}{\hbar}\left\langle\sum_{k,\sigma}\{V_{\eta\sigma}c_{\eta k\sigma}^\dagger(t)[e^\dagger(t)f_\sigma(t)+\sigma f_{\bar{\sigma}}^\dagger(t)d(t)]\right. \\
&\quad\left. -V_{\eta\sigma}^*[f_\sigma^\dagger(t)e(t)+\sigma d^\dagger f_{\bar{\sigma}}(t)]c_{\eta k\sigma}(t)\}\right\rangle. \quad (13)
\end{aligned}
$$

Ultimately, the current can be expressed in terms of the GF's in the QD:

$$
\begin{aligned}
I_\eta = ie\int\frac{d\omega}{2\pi}\sum_\sigma\{\Gamma_{\eta\sigma}f_\eta(\omega)[G_{e\sigma\sigma}^>(\omega)+G_{d\bar{\sigma}\bar{\sigma}}^>(\omega)] \\
+\Gamma_{\eta\sigma}[1-f_\eta(\omega)][G_{e\sigma\sigma}^<(\omega)+G_{d\bar{\sigma}\bar{\sigma}}^<(\omega)]\}. \quad (14)
\end{aligned}
$$

Under the weak-coupling approximation, it becomes

$$
I_\eta/e = \sum_\sigma(\tilde{\Gamma}_{\eta\sigma}^-\rho_{dd}+\Gamma_{\eta\sigma}^-\rho_{\sigma\sigma}-\tilde{\Gamma}_{\eta\bar{\sigma}}^+\rho_{\sigma\sigma}-\Gamma_{\eta\sigma}^+\rho_{00}). \quad (15)
$$

This formula demonstrates that all possible tunneling processes relevant to the lead η can provide corresponding contributions to the current of the lead η and the current is totally determined by the diagonal elements of the density-matrix of the central region. However, the nondiagonal element of the density-matrix is coupled with diagonal elements in the rate equation (12b), and therefore influences the tunneling current indirectly.

C. Discussion

The rate equations (12) may be readily solved under stationary condition for arbitrary bias voltages V and temperatures T, and consequently the dc current may be obtained via Eq. (15). More interestingly, it is useful to review the following two special cases in the case of large Coulomb repulsion. First, we consider that no doubly occupied state is available in the QD, i.e., $\rho_{dd}=0$. In this case, we assume that the bare level ϵ_d of the QD is just above the Fermi levels μ of the two leads under equilibrium condition, meaning $\tilde{\Gamma}_\sigma^+\simeq0$, $\tilde{\Gamma}_\sigma^-\simeq\Sigma_\eta\Gamma_{\eta\sigma}$. Then, in steady state, the quantum rate equations (12b) and (12c) become

$$
\Gamma_\sigma^+\rho_{00}-\Gamma_\sigma^-\rho_{\sigma\sigma}-2\mathrm{Im}(R_{\bar{\sigma}}\rho_{\sigma\bar{\sigma}})=0, \quad (16a)
$$

$$
iR_\sigma(\rho_{\sigma\sigma}-\rho_{\bar{\sigma}\bar{\sigma}})-\frac{1}{2}(\Gamma_\sigma^-+\Gamma_{\bar{\sigma}}^-)\rho_{\sigma\bar{\sigma}}=0, \quad (16b)
$$

with $\rho_{00}+\Sigma_\sigma\rho_{\sigma\sigma}=1$. They can be readily solved

$$
\rho_{\uparrow\uparrow}=\frac{\Gamma_\uparrow^+\Gamma_\downarrow^-+\chi(\Gamma_\uparrow^++\Gamma_\downarrow^+)}{\Delta}, \quad (17a)
$$

$$
\rho_{\downarrow\downarrow}=\frac{\Gamma_\downarrow^+\Gamma_\uparrow^-+\chi(\Gamma_\uparrow^++\Gamma_\downarrow^+)}{\Delta}, \quad (17b)
$$

in which $\Delta=[(\Gamma_\uparrow^++\Gamma_\uparrow^-)(\Gamma_\downarrow^++\Gamma_\downarrow^-)-\Gamma_\uparrow^+\Gamma_\downarrow^+]+\chi(2\Gamma_\uparrow^+ +2\Gamma_\downarrow^++\Gamma_\uparrow^-+\Gamma_\downarrow^-)$ and $\chi=4|R|^2/(\Gamma_\uparrow^-+\Gamma_\downarrow^-)$. The steady tunneling current is $I_R=e\Sigma_\sigma[(\Gamma_{R\sigma}^++\Gamma_{R\bar{\sigma}}^++\Gamma_{R\sigma}^-)\rho_{\sigma\sigma} -\Gamma_{R\sigma}^+]$. For large bias voltage, i.e., $\Gamma_{L\sigma}^-=0$ and $\Gamma_{R\sigma}^+=0$, and spin-independent tunneling, the dc current becomes

$$
I_R/e = \frac{2\Gamma_L(\Gamma_R+2\chi')}{2\Gamma_L+\Gamma_R+\chi'(2+4\Gamma_L/\Gamma_R)}, \quad (18)
$$

and $\chi'=2|R|^2/\Gamma_R$, which depicts the spin-flip transition induced modification for the corresponding formula, Eq. (3.10) in Ref. 15.

The second case we consider here is the deep level in the large-U limit: the bare level ϵ_d is far below the Fermi level μ but ϵ_d+U is slightly above the Fermi level in equilibrium condition, implicating that the QD is always occupied by electrons. In this situation, we have $\rho_{00}=0$, $\Gamma_\sigma^-\simeq0$, and $\Gamma_\sigma^+\simeq\Sigma_\eta\Gamma_{\eta\sigma}$. Different from the above case, only singly and doubly occupied states are permitted in tunneling processes. Under the stationary condition, the quantum rate equations (12b) and (12c) reduce to

$$
\tilde{\Gamma}_{\bar{\sigma}}^-\rho_{dd}-\tilde{\Gamma}_{\bar{\sigma}}^+\rho_{\sigma\sigma}-2\mathrm{Im}(R_{\bar{\sigma}}\rho_{\sigma\bar{\sigma}})=0, \quad (19a)
$$

$$
iR_\sigma(\rho_{\sigma\sigma}-\rho_{\bar{\sigma}\bar{\sigma}})-\tfrac{1}{2}(\tilde{\Gamma}_\sigma^++\tilde{\Gamma}_{\bar{\sigma}}^+)\rho_{\sigma\bar{\sigma}}=0, \quad (19b)
$$

with $\rho_{dd}+\Sigma_\sigma\rho_{\sigma\sigma}=1$. The solutions are

$$
\rho_{\uparrow\uparrow}=\left[\frac{(\tilde{\Gamma}_\uparrow^++\chi)(\tilde{\Gamma}_\downarrow^++\tilde{\Gamma}_\downarrow^-)+\chi(\tilde{\Gamma}_\uparrow^++\tilde{\Gamma}_\uparrow^-)}{(\tilde{\Gamma}_\uparrow^++\chi)(\tilde{\Gamma}_\downarrow^++\chi)-\chi^2}-1\right]\rho_{dd}, \quad (20a)
$$

$$\rho_{\downarrow\downarrow} = \left[\frac{(\tilde{\Gamma}_{\downarrow}^{+} + \chi)(\tilde{\Gamma}_{\uparrow}^{+} + \tilde{\Gamma}_{\uparrow}^{-}) + \chi(\tilde{\Gamma}_{\uparrow}^{+} + \tilde{\Gamma}_{\downarrow}^{-})}{(\tilde{\Gamma}_{\uparrow}^{+} + \chi)(\tilde{\Gamma}_{\downarrow}^{+} + \chi) - \chi^{2}} - 1 \right] \rho_{dd},$$

(20b)

$$\rho_{dd} = \left[\frac{(\tilde{\Gamma}_{\downarrow}^{+} + \chi)(\tilde{\Gamma}_{\uparrow}^{+} + \tilde{\Gamma}_{\uparrow}^{-}) + \chi(\tilde{\Gamma}_{\downarrow}^{+} + \tilde{\Gamma}_{\downarrow}^{-})}{(\tilde{\Gamma}_{\downarrow}^{+} + \chi)\tilde{\Gamma}_{\uparrow}^{+} + \chi\tilde{\Gamma}_{\downarrow}^{+}} \right.$$
$$\left. + \frac{(\tilde{\Gamma}_{\uparrow}^{+} + \chi)(\tilde{\Gamma}_{\downarrow}^{+} + \tilde{\Gamma}_{\downarrow}^{-}) + \chi(\tilde{\Gamma}_{\uparrow}^{+} + \tilde{\Gamma}_{\uparrow}^{-})}{(\tilde{\Gamma}_{\uparrow}^{+} + \chi)\tilde{\Gamma}_{\downarrow}^{+} + \chi\tilde{\Gamma}_{\uparrow}^{+}} - 1 \right]^{-1},$$

(20c)

with $\chi = 4|R|^2/(\tilde{\Gamma}_{\uparrow}^{+} + \tilde{\Gamma}_{\downarrow}^{+})$. The steady tunneling current is given by $I_R = e\sum_{\sigma}[\tilde{\Gamma}_{R\sigma}^{-}\rho_{dd} - \tilde{\Gamma}_{R\sigma}^{+}\rho_{\sigma\sigma}]$. Large bias voltage further simplifies the spin-independent current as

$$I_R/e = \frac{2\tilde{\Gamma}_L \tilde{\Gamma}_R + 2\chi''}{\tilde{\Gamma}_L + 2\tilde{\Gamma}_R + 2\chi''(1 + \tilde{\Gamma}_R/\tilde{\Gamma}_L)},$$

(21)

with $\chi'' = 2|R|^2/\tilde{\Gamma}_L$. This is a modification of Eq. (3.11) given by Gurvitz and Prager due to spin-flip transitions.[15]

It should be noted that the same two cases are also analyzed in Ref. 35 for an interacting QD with spin-flip transitions included. They evaluated the occupation numbers from the classical rate equations and utilized a spin-relaxation time τ_s to describe the spin-flip transitions. Therefore, their results are slightly different from ours. For both cases, if we redefine the spin-relaxation time τ_s as $1/\tau_s = \chi$, which is now of temperature and bias voltage dependence, their results[35] are the same as ours, Eqs. (17) and (20) of the quantum rate equations. This is a clear demonstration of the importance of quantum "coherence."

It is also worth examining the quantum rate equations (12) derived here at large bias voltage between the left and right leads without the spin-flip transitions. In this case, we assume $eV \gg T$ and $eV \gg U$, so $\Gamma_{L\sigma}^{-} = \Gamma_{R\sigma}^{+} = 0$ and $\tilde{\Gamma}_{L\sigma}^{-} = \tilde{\Gamma}_{R\sigma}^{+} = 0$. The quantum rate equations lead to the following:

$$\dot{\rho}_{00} = \Gamma_{R\uparrow}\rho_{\uparrow\uparrow} + \Gamma_{R\downarrow}\rho_{\downarrow\downarrow} - (\Gamma_{L\uparrow} + \Gamma_{L\downarrow})\rho_{00},$$

(22a)

$$\dot{\rho}_{\sigma\sigma} = \Gamma_{L\sigma}\rho_{00} + \tilde{\Gamma}_{R\bar{\sigma}}\rho_{dd} - (\Gamma_{R\sigma} + \tilde{\Gamma}_{L\bar{\sigma}})\rho_{\sigma\sigma},$$

(22b)

$$\dot{\rho}_{dd} = \tilde{\Gamma}_{L\downarrow}\rho_{\uparrow\uparrow} + \tilde{\Gamma}_{L\uparrow}\rho_{\downarrow\downarrow} - (\tilde{\Gamma}_{R\uparrow} + \tilde{\Gamma}_{R\downarrow})\rho_{dd},$$

(22c)

and the current is $I_R = e\sum_{\sigma}(\tilde{\Gamma}_{R\bar{\sigma}}\rho_{dd} + \Gamma_{R\sigma}\rho_{\sigma\sigma})$. At zero temperature and spin-independent tunneling, these equations indeed resemble the rate equations derived from the Schrödinger equation developed by Gurvitz and Prager.[15]

D. Numerical results

In this section, we perform numerical calculations for the spin dependence of the tunneling processes through the SQD connected to two ferromagnetic leads. In the following calculations, we consider two magnetic configurations, namely, parallel (P) and antiparallel (AP) configurations. When the magnetic electrodes are in P configuration, we assume that the majority electrons are spin up $\sigma = \uparrow$ and the minority

electrons are spin down $\sigma = \downarrow$. We also assume that in the AP configuration the magnetization of the right electrode is reversed.

Therefore, for the identical leads and symmetric barriers, of interest in the present paper, we further assume that the ferromagnetism of the leads can be accounted for by the polarization-dependent couplings $\Gamma_{L\uparrow} = \Gamma_{R\uparrow} = (1+p)\Gamma_0$, $\Gamma_{L\downarrow} = \Gamma_{R\downarrow} = (1-p)\Gamma_0$ for the P alignment, while $\Gamma_{L\uparrow} = \Gamma_{R\downarrow} = (1+p)\Gamma_0$, $\Gamma_{L\downarrow} = \Gamma_{R\uparrow} = (1-p)\Gamma_0$ for the AP alignment. Γ_0 denotes the tunneling coupling between the QD and the leads without internal magnetization, and p ($0 \leq p < 1$) stands for the polarization strength of the leads. In the wide band limit, Γ_0 is supposed to be a constant and chosen as unit of energy in the following paper. Moreover, we measure energy from the Fermi levels of the left and right leads in the equilibrium condition ($\mu_L = \mu_R = 0$) thereafter. The discrete level ϵ_d of the QD can cross the Fermi levels by tuning the gate voltage in experiments. Without loss of generality, we apply the bias voltage V between the source and drain symmetrically $\mu_L = -\mu_R = eV/2$, and neglect the shift of the discrete level caused by this external voltage. Because of the symmetry, we will restrict to positive bias only, $V > 0$.

From Eqs. (12), one can find all the expectation values of the density-matrix elements for a given bias V in the stationary condition, and thus allow us to calculate the tunneling current flowing through the system by employing Eq. (15) and the nonequilibrium occupation numbers $n_{\uparrow}$, $n_{\downarrow}$, defined by $n_{\sigma} = \rho_{\sigma\sigma} + \rho_{dd}$.

First we consider no spin-flip scattering processes on the QD. Figures 2(a) and 2(b) plot the nonequilibrium occupation numbers as a function of the bare level calculated for a small bias $V = 1.0$ and a large bias $V = 10.0$, respectively, in both P (thin lines) and AP (thick lines) configurations. The two spacial bias voltages are chosen in order here to demonstrate the linear-response regime ($V = 1.0$) and the strong nonlinear case ($V = 10.0$), respectively. For comparison, we also plot the equilibrium occupation numbers in Fig. 2(b). From these figures, we can observe the following: (1) The complete Coulomb blockade (charging) effect in equilibrium (the single step in ρ_{dd}) is partially removed in nonequilibrium, i.e., ρ_{dd} becomes a multistep function of the gate voltage; (2) n_{σ} has fractional steps in nonequilibrium in contrast to just half-integer steps in equilibrium; (3) $n_{\uparrow} = n_{\downarrow}$ in the P configuration, whereas $n_{\uparrow} \neq n_{\downarrow}$ in the AP configuration. Figure 2(c) shows the tunneling current calculated for both configurations. The current in the P alignment is always larger than that in the AP alignment in the whole range of the gate voltage. In the linear-response regime, the current provides the information of the conductance of the device: there appear two resonant peaks with equal heights when the gate voltage controlled levels ϵ_d and $\epsilon_d + U$, respectively, cross the Fermi levels of two leads. While in the strong nonequilibrium case, there are three steps in the current which correspond to the steps in the occupation numbers, whereas between the steps the current is constant.

Figure 3 illustrates typical variations of the occupation numbers and the current with the bias voltage V for $\epsilon_d = 1$ (the no doubly occupied level) and $\epsilon_d = -5$ (the deep level). In the first (second) case, the first step in n_{σ} occurs at the
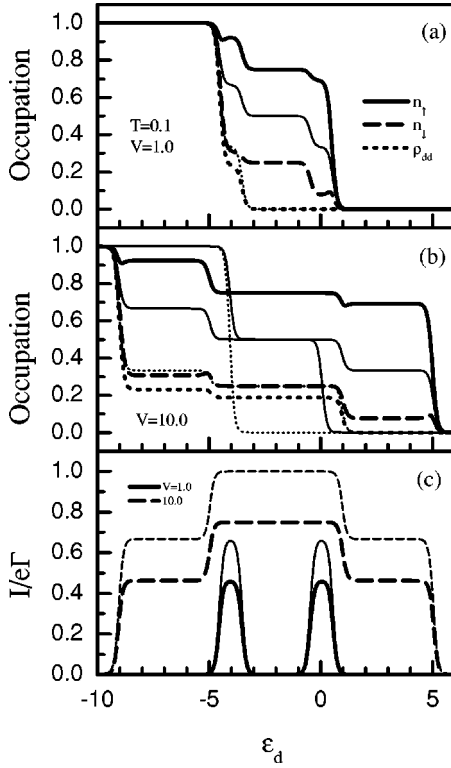
FIG. 2. Nonequilibrium occupation numbers $n_\uparrow$, $n_\downarrow$, and ρ_{dd} (a,b), and tunneling current (c) vs the bare level of the SQD with no spin-flip scattering for both magnetization configurations. (a) is plotted at a small bias $V=1.0$ and (b) is at a large bias $V=10.0$. The thick lines are plotted for the AP configuration, and the thin curves are for the P configuration. The equilibrium occupation numbers are depicted by the thin lines in (b). Other parameters are $U=4$, $T=0.1$, and $p=0.5$.

FIG. 3. Occupation numbers $n_\uparrow$, $n_\downarrow$ (a,d), ρ_{dd} (b,e), and current (c,f) vs the bias voltage, calculated for no spin-flip processes and different temperatures $T=0.1$, 0.5, and 1.0. (a)–(c) are plotted for $\epsilon_d=1$ and (d)–(f) for $\epsilon_d=-5$. Insets in (c) and (f): the corresponding TMR vs the bias voltage. Other parameters are as in Fig. 2.

bias, when the Fermi level of the source or drain crosses the discrete level ϵ_d (ϵ_d+U). This means a new channel opens for tunneling. Consequently, we find that a step in the current appears at this position. As the bias further increases, they all keep constant until the second step at a higher voltage corresponding to the case when the Fermi level crosses $\epsilon_d+U(\epsilon_d)$, which also induces a step in ρ_{dd}. The insets in Fig. 3(c) and 3(f) depict the corresponding tunnel magnetoresistance (TMR), defined as

$$\text{TMR} \equiv \frac{I_\text{P}-I_\text{AP}}{I_\text{AP}}. \qquad (23)$$

The TMR is enhanced by the Coulomb interaction in the range between the two biases corresponding to the two steps in the current. In these figures, we also display the temperature effect in tunneling characteristics. It is easily observed that increasing temperature gradually smoothes the steep step structure in the occupation numbers and the current, and decreases the TMR.

We now consider the effect of spin-flip scatterings on tunneling. Because the spin-flip processes have no influence on the occupation numbers and the current in the P configuration, we plot the calculated results for the AP configuration
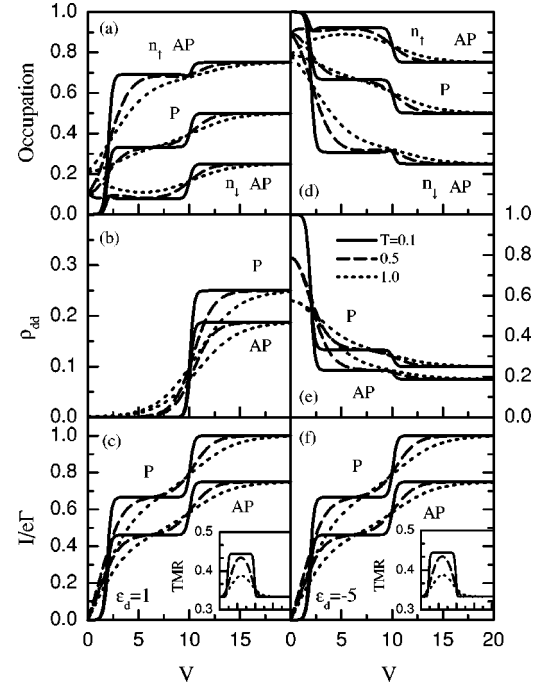
with $R=1$ in Fig. 4. It is obvious, in comparison with the case of no spin-flip scattering $R=0$ (thin lines), that the spin-flip transition decreases the difference between $n_\uparrow$ and $n_\downarrow$, increases ρ_{dd} and the current. Moreover, their temperature behaviors are similar to the case of no spin-flip transition. It is worth noting that when the bias voltage is lower than 10.0, i.e., the value corresponding to the second step in n_σ and the only step in ρ_{dd}, we have approximately $\rho_{dd}\simeq0$ (no doubly occupied level) for $\epsilon_d=1$ and $\rho_{00}\simeq0$ (deep level) for $\epsilon_d=-5$, indicating that Eqs. (17) and (20) are valid in this bias range. Therefore, we can utilize the definition of the spin relaxation rate in these equations to account for the importance of temperature and bias on the spin-flip scattering, as depicted in the insets of Figs. 4(b) and 4(e).

III. COUPLED QUANTUM DOTS

Now we turn to resonant tunneling through a CQD with weak coupling between the QD's and the leads, as shown in Fig. 1(b). The presumption that the interdot hopping is also weak keeps each level of the dots isolated. Then the superposition of the two levels in different QD's plays a crucial role in tunneling. In order to simplify our derivation, we consider here the infinite intradot Coulomb repulsion U' and a finite interdot Coulomb interaction U, which excludes the state of two electrons in the same QD but two electrons can occupy different QD's.
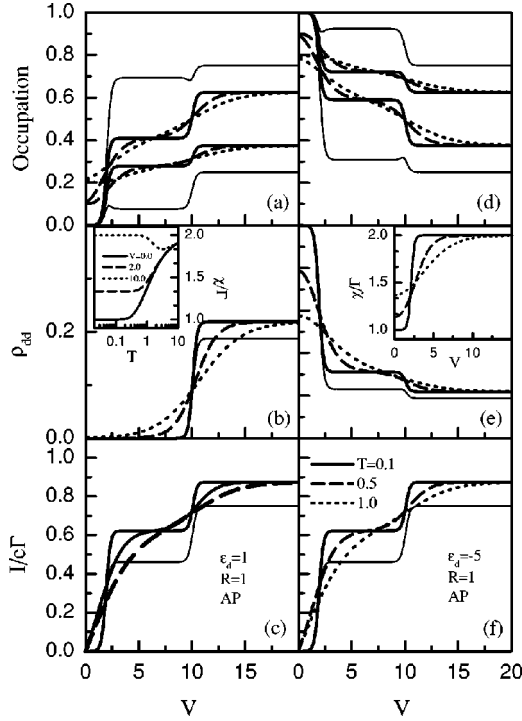
FIG. 4. Occupation numbers $n_\uparrow$, $n_\downarrow$ (a,d), ρ_{dd} (b,e), and current (c,f) vs the bias voltage calculated for the AP configuration with the spin-flip transition $R=1$ and different temperatures $T=0.1$, 0.5, and 1.0. (a)–(c) are plotted for $\epsilon_d=1$ and (d)–(f) for $\epsilon_d=-5$. For comparison, the respective results without the spin-flip transition are also plotted as thin lines. Insets in (b) and (e): the temperature and bias dependence of the spin relaxation rate. Other parameters are as in Fig. 2.

A. Model Hamiltonian and slave-particle representation

The tunneling Hamiltonian for the CQD is

$$H = \sum_{\eta,k,\sigma} \epsilon_{\eta k \sigma} c_{\eta k \sigma}^\dagger c_{\eta k \sigma} + \epsilon_1 \sum_\sigma c_{1\sigma}^\dagger c_{1\sigma} + \epsilon_2 \sum_\sigma c_{2\sigma}^\dagger c_{2\sigma}$$

$$+ t \sum_\sigma (c_{1\sigma}^\dagger c_{2\sigma} + c_{2\sigma}^\dagger c_{1\sigma}) + U' n_{1\uparrow} n_{1\downarrow} + U' n_{2\uparrow} n_{2\downarrow}$$

$$+ U \sum_{\sigma,\sigma'} n_{1\sigma} n_{2\sigma'} + \sum_{k,\sigma} (V_{L\sigma} c_{Lk\sigma}^\dagger c_{1\sigma} + \text{H.c.})$$

$$+ \sum_{k,\sigma} (V_{R\sigma} c_{Rk\sigma}^\dagger c_{2\sigma} + \text{H.c.}), \qquad (24)$$

where $c_{1(2)\sigma}^\dagger$ and $c_{1(2)\sigma}$ are creation and annihilation operators for a spin-σ electron in the first (second) QD, respectively. ϵ_j ($j=1,2$) is the bare-level energy of electrons in the jth QD, $\epsilon_{1(2)} = \epsilon_d \pm \delta$, in which δ is the bare mismatch between the two bare levels. The first term in the second line denotes the hopping t between the two QD's. The other notations are the same as those in Sec. II.

In the situation discussed here, the bare mismatch δ should be very small. Otherwise, the quantum coherence (the superposition of the two states) has quite tiny effect on the tunneling processes. In experiments, this small mismatch

could be controlled by external time-dependent voltages. The available states and the corresponding energies for the isolated CQD are the following: (1) the whole system is empty, $|0\rangle_1|0\rangle_2$, and the energy is zero; (2) the first QD is singly occupied, $|\sigma\rangle_1|0\rangle_2$, and the energy is ϵ_1; (3) the second QD is singly occupied, $|0\rangle_1|\sigma\rangle_2$, and the energy is ϵ_2; and (4) both of the QD's are singly occupied, $|\sigma\rangle_1|\sigma'\rangle_2$, and the energy is $2\epsilon_d + U$. With the same theoretical point of view as in the single QD mentioned in the above section, we can decompose the real electron operator $c_{j\sigma}$ in these Fock states as

$$c_{1\sigma} = |0\rangle_1|0\rangle_{22}\langle 0|_1\langle \sigma| + \sum_{\sigma'} |0\rangle_1|\sigma'\rangle_{22}\langle \sigma'|_1\langle \sigma|, \quad (25)$$

$$c_{2\sigma} = |0\rangle_1|0\rangle_{22}\langle 0|_1\langle \sigma| + \sum_{\sigma'} |\sigma'\rangle_1|0\rangle_{22}\langle \sigma|_1\langle \sigma'|, \quad (26)$$

in association with the completeness relation

$$|0\rangle_1|0\rangle_{22}\langle 0|_1\langle 0| + \sum_{\sigma,\sigma'} |\sigma\rangle_1|\sigma'\rangle_{22}\langle \sigma'|_1\langle \sigma|$$

$$+ \sum_\sigma (|\sigma\rangle_1|0\rangle_{22}\langle 0|\langle \sigma| + |0\rangle_1|\sigma\rangle_{22}\langle \sigma|_1\langle 0|) = 1.$$

$$(27)$$

Again, we assign these Dirac brackets as operators: the slave-boson operators $e^\dagger = |0\rangle_1|0\rangle_2$, $d_{\sigma\sigma'}^\dagger = |\sigma\rangle_1|\sigma'\rangle_2$ and the pseudofermion operators $f_{1\sigma}^\dagger = |\sigma\rangle_1|0\rangle_2$, $f_{2\sigma}^\dagger = |0\rangle_1|\sigma\rangle_2$. Then, Eqs. (25)–(27) can be replaced as

$$c_{1\sigma} = e^\dagger f_{1\sigma} + \sum_{\sigma'} f_{2\sigma'}^\dagger d_{\sigma\sigma'}, \qquad (28)$$

$$c_{2\sigma} = e^\dagger f_{2\sigma} + \sum_{\sigma'} f_{1\sigma'}^\dagger d_{\sigma'\sigma}, \qquad (29)$$

$$e^\dagger e + \sum_\sigma (f_{1\sigma}^\dagger f_{1\sigma} + f_{2\sigma}^\dagger f_{2\sigma}) + \sum_{\sigma\sigma'} d_{\sigma\sigma'}^\dagger d_{\sigma\sigma'} = 1. \quad (30)$$

And obviously the explicit (anti)communicators of these auxiliary particles are

$$ee^\dagger = 1, \quad d_{\sigma_1\sigma_2} d_{\sigma_1'\sigma_2'}^\dagger = \delta_{\sigma_1\sigma_1'}\delta_{\sigma_2\sigma_2'}, \quad f_{i\sigma}f_{j\sigma'}^\dagger = \delta_{ij}\delta_{\sigma\sigma'},$$

$$ed_{\sigma\sigma'}^\dagger = ef_{j\sigma}^\dagger = f_{j\sigma}e^\dagger = f_{j\sigma}d_{\sigma'\sigma''}^\dagger = d_{\sigma\sigma'}e^\dagger = d_{\sigma'\sigma''}f_{j\sigma}^\dagger = 0.$$

$$(31)$$

The density-matrix elements are expressed as

$$\hat{\rho}_{00} = |0\rangle_1|0\rangle_{22}\langle 0|_1\langle 0| = e^\dagger e,$$

$$\hat{\rho}_{11\sigma} = |\sigma\rangle_1|0\rangle_{22}\langle 0|_1\langle \sigma| = f_{1\sigma}^\dagger f_{1\sigma},$$

$$\hat{\rho}_{22\sigma} = |0\rangle_1|\sigma\rangle_{22}\langle \sigma|_1\langle 0| = f_{2\sigma}^\dagger f_{2\sigma},$$

$$\hat{\rho}_{dd\sigma\sigma'} = |\sigma\rangle_1|\sigma'\rangle_{22}\langle \sigma'|_1\langle \sigma| = d_{\sigma\sigma'}^\dagger d_{\sigma\sigma'},$$

and

$$\hat{\rho}_{12\sigma} = |0\rangle_1|\sigma\rangle_{22}\langle 0|_1\langle \sigma| = f_{2\sigma}^\dagger f_{1\sigma}.$$

In terms of these slave-particle operators, the Hamiltonian for the CQD can be rewritten as

$$H = \sum_{\eta,k,\sigma} \epsilon_{\eta k \sigma} c^{\dagger}_{\eta k \sigma} c_{\eta k \sigma} + \epsilon_1 \sum_{\sigma} f^{\dagger}_{1\sigma} f_{1\sigma} + \epsilon_2 \sum_{\sigma} f^{\dagger}_{2\sigma} f_{2\sigma} + t \sum_{\sigma} (f^{\dagger}_{1\sigma} f_{2\sigma} + f^{\dagger}_{2\sigma} f_{1\sigma})$$

$$+ (2\epsilon_d + U) \sum_{\sigma,\sigma'} d^{\dagger}_{\sigma\sigma'} d_{\sigma\sigma'} + \sum_{k,\sigma} \left[V_{L\sigma} c^{\dagger}_{Lk\sigma} \left(e^{\dagger} f_{1\sigma} + \sum_{\sigma'} f^{\dagger}_{2\sigma'} d_{\sigma\sigma'} \right) + \text{H.c.} \right]$$

$$+ \sum_{k,\sigma} \left[V_{R\sigma} c^{\dagger}_{Rk\sigma} \left(e^{\dagger} f_{2\sigma} + \sum_{\sigma'} f^{\dagger}_{1\sigma'} d_{\sigma'\sigma} \right) + \text{H.c.} \right]. \tag{32}$$

B. The quantum rate equations for the CQD

Define the retarded (advanced) and lesser (greater) GF's for the CQD $G^{r(a),<(>)}_{ij\sigma}(t,t') \equiv \langle\langle c_{i\sigma}(t) | c^{\dagger}_{j\sigma}(t') \rangle\rangle^{r(a),<(>)}$ as usual. Considering Eqs. (25) and (26), these GFs can be expressed in terms of the slave particles: $G_{ij\sigma} = G_{eij\sigma} + \Sigma_{\sigma'\sigma''} G_{d\bar{i}j\sigma\sigma'\sigma''}$ [$\bar{i}=2(1)$ if $i=1(2)$] with $G_{eij\sigma} \equiv \langle\langle e^{\dagger}(t) f_{i\sigma}(t) | f^{\dagger}_{j\sigma}(t') e(t') \rangle\rangle$ and $G_{d11\sigma\sigma'\sigma''} = \langle\langle f^{\dagger}_{1\sigma'}(t) d_{\sigma'\sigma}(t) | d^{\dagger}_{\sigma''\sigma}(t') f_{1\sigma''}(t') \rangle\rangle$, $G_{d22\sigma\sigma'\sigma''} = \langle\langle f^{\dagger}_{2\sigma'}(t) d_{\sigma\sigma'}(t) | d^{\dagger}_{\sigma\sigma''}(t') f_{2\sigma''}(t') \rangle\rangle$. In the following derivation, we will use the nondiagonal doubly occupied related GF's, for example, $G_{d21\sigma\sigma'\sigma''} = \langle\langle f^{\dagger}_{2\sigma'}(t) d_{\sigma'\sigma''}(t) | d^{\dagger}_{\sigma'\sigma}(t') f_{1\sigma}(t') \rangle\rangle$ and $G'_{d21\sigma\sigma'\sigma''} = \langle\langle f^{\dagger}_{2\sigma}(t) d_{\sigma\sigma'}(t) | d^{\dagger}_{\sigma''\sigma'}(t') f_{1\sigma''}(t') \rangle\rangle$. Under the weak-coupling assumption and small bare detuning δ, the decoupled GF's of the CQD can be defined in terms of spectrum expressions, in the Fourier space, as

$$G^{<0}_{eii\sigma}(\omega) = 2\pi i \rho_{ii\sigma} \delta(\omega - \epsilon_d),$$

$$G^{<0}_{d11\sigma\sigma'\sigma''}(\omega) = \delta_{\sigma'\sigma''} 2\pi i \rho_{dd\sigma'\sigma} \delta[\omega - (\epsilon_d + U)],$$

$$G^{<0}_{d22\sigma\sigma'\sigma''}(\omega) = \delta_{\sigma'\sigma''} 2\pi i \rho_{dd\sigma\sigma'} \delta[\omega - (\epsilon_d + U)],$$

$$G^{>0}_{eii\sigma}(\omega) = -2\pi i \rho_{00} \delta(\omega - \epsilon_d), G^{>0}_{dii\sigma\sigma'\sigma''}(\omega)$$

$$= -\delta_{\sigma'\sigma''} 2\pi i \rho_{ii\sigma'} \delta[\omega - (\epsilon_d + U)], \tag{33}$$

$$G^{(')<0}_{dij\sigma\sigma'\sigma''}(\omega) = 0, \quad G^{>0}_{eij\sigma}(\omega) = 0,$$

$$G^{<0}_{eij\sigma}(\omega) = 2\pi i \rho_{ij\sigma} \delta(\omega - \epsilon_d),$$

$$G^{(')>0}_{dij\sigma\sigma'\sigma''}(\omega) = -\delta_{\sigma\sigma''} 2\pi i \rho_{ji\sigma} \delta[\omega - (\epsilon_d + U)]. \tag{34}$$

In order to get the quantum rate equations, we use exactly the same procedure as in the preceding section, evaluating the statistical expectations of the rate of time change of the density-matrix elements ρ_{ij}. After tedious but straightforward calculations, eventually we obtain in the wide band limit

$$\dot{\rho}_{00} = -\frac{i}{2\pi} \int d\omega \sum_{\sigma} \{ \Gamma_{L\sigma} f_L(\omega) G^{>}_{e11\sigma}(\omega)$$

$$+ \Gamma_{L\sigma} [1 - f_L(\omega)] G^{<}_{e11\sigma}(\omega) + \Gamma_{R\sigma} f_R(\omega) G^{>}_{e22\sigma}(\omega)$$

$$+ \Gamma_{R\sigma} [1 - f_R(\omega)] G^{<}_{e22\sigma}(\omega) \}, \tag{35a}$$

$$\dot{\rho}_{11\sigma} = \frac{i}{2\pi} \int d\omega \left\{ \Gamma_{L\sigma} f_L(\omega) G^{>}_{e11\sigma}(\omega) + \Gamma_{L\sigma} [1 \right.$$

$$- f_L(\omega)] G^{<}_{e11\sigma}(\omega) - \sum_{\sigma',\sigma''} \Gamma_{R\sigma'} f_R(\omega) G^{>}_{d11\sigma'\sigma\sigma''}(\omega)$$

$$\left. - \sum_{\sigma',\sigma''} \Gamma_{R\sigma'} [1 - f_R(\omega)] G^{<}_{d11\sigma'\sigma\sigma''}(\omega) \right\}$$

$$+ it(\rho_{12\sigma} - \rho_{21\sigma}), \tag{35b}$$

$$\dot{\rho}_{22\sigma} = \frac{i}{2\pi} \int d\omega \left\{ \Gamma_{R\sigma} f_R(\omega) G^{>}_{e22\sigma}(\omega) + \Gamma_{R\sigma} [1 \right.$$

$$- f_R(\omega)] G^{<}_{e22\sigma}(\omega) - \sum_{\sigma',\sigma''} \Gamma_{L\sigma'} f_L(\omega) G^{>}_{d22\sigma'\sigma\sigma''}(\omega)$$

$$\left. - \sum_{\sigma',\sigma''} \Gamma_{L\sigma'} [1 - f_L(\omega)] G^{<}_{d22\sigma'\sigma\sigma''}(\omega) \right\}$$

$$+ it(\rho_{21\sigma} - \rho_{12\sigma}), \tag{35c}$$

$$\dot{\rho}_{12\sigma} = i(\epsilon_2 - \epsilon_1)\rho_{12\sigma} + \frac{i}{4\pi} \int d\omega \left\{ \sum_{\eta} \{ \Gamma_{\eta\sigma} f_{\eta}(\omega) G^{>}_{e12\sigma}(\omega) \right.$$

$$+ \Gamma_{\eta\sigma} [1 - f_{\eta}(\omega)] G^{<}_{e12\sigma}(\omega) \}$$

$$- \sum_{\sigma',\sigma''} \{ \Gamma_{L\sigma'} f_L(\omega) G^{>}_{d21\sigma\sigma'\sigma''}(\omega)$$

$$+ \Gamma_{L\sigma'} [1 - f_L(\omega)] G^{<}_{d21\sigma\sigma'\sigma''}(\omega) \}$$

$$- \sum_{\sigma',\sigma''} \{ \Gamma_{R\sigma'} f_R(\omega) G'^{>}_{d21\sigma\sigma'\sigma''}(\omega)$$

$$\left. + \Gamma_{R\sigma'} [1 - f_R(\omega)] G'^{<}_{d21\sigma\sigma'\sigma''}(\omega) \} \right\}$$

$$+ it(\rho_{11\sigma} - \rho_{22\sigma}), \tag{35d}$$

$$\dot{\rho}_{dd\sigma\sigma} = \frac{i}{2\pi} \int d\omega \sum_{\sigma'} \{ \Gamma_{L\sigma} f_L(\omega) G^>_{d22\sigma\sigma\sigma'}(\omega)$$

$$+ \Gamma_{L\sigma}[1 - f_L(\omega)] G^<_{d22\sigma\sigma\sigma'}(\omega)$$

$$+ \Gamma_{R\sigma} f_R(\omega) G^>_{d11\sigma\sigma\sigma'}(\omega)$$

$$+ \Gamma_{R\sigma}[1 - f_R(\omega)] G^<_{d11\sigma\sigma\sigma'}(\omega) \}, \tag{35e}$$

$$\dot{\rho}_{dd\sigma\bar{\sigma}} = \frac{i}{2\pi} \int d\omega \sum_{\sigma'} \{ \Gamma_{L\sigma} f_L(\omega) G^>_{d22\bar{\sigma}\bar{\sigma}\sigma'}(\omega)$$

$$+ \Gamma_{L\sigma}[1 - f_L(\omega)] G^<_{d22\bar{\sigma}\bar{\sigma}\sigma'}(\omega)$$

$$+ \Gamma_{R\bar{\sigma}} f_R(\omega) G^>_{d11\bar{\sigma}\sigma\sigma'}(\omega) + \Gamma_{R\bar{\sigma}}[1$$

$$- f_R(\omega)] G^<_{d11\bar{\sigma}\sigma\sigma'}(\omega) \}. \tag{35f}$$

Substituting these correlation GF's with their decoupled formulations, Eqs. (33) and (34), the quantum rate equations can be obtained as

$$\dot{\rho}_{00} = \sum_{\sigma} [\Gamma^-_{L\sigma}\rho_{11\sigma} + \Gamma^-_{R\sigma}\rho_{22\sigma} - (\Gamma^+_{L\sigma} + \Gamma^+_{R\sigma})\rho_{00}], \tag{36a}$$

$$\dot{\rho}_{11\sigma} = \Gamma^+_{L\sigma}\rho_{00} + \sum_{\sigma'} \tilde{\Gamma}^-_{R\sigma'}\rho_{dd\sigma\sigma'} - \Gamma^-_{L\sigma}\rho_{11\sigma}$$

$$- \sum_{\sigma'} \tilde{\Gamma}^+_{R\sigma'}\rho_{11\sigma} - 2t\mathrm{Im}\rho_{12\sigma}, \tag{36b}$$

$$\dot{\rho}_{22\sigma} = \Gamma^+_{R\sigma}\rho_{00} + \sum_{\sigma'} \tilde{\Gamma}^-_{L\sigma'}\rho_{dd\sigma'\sigma} - \Gamma^-_{R\sigma}\rho_{22\sigma}$$

$$- \sum_{\sigma'} \tilde{\Gamma}^+_{L\sigma'}\rho_{22\sigma} + 2t\mathrm{Im}\rho_{12\sigma}, \tag{36c}$$

$$\dot{\rho}_{12\sigma} = i(\epsilon_2 - \epsilon_1)\rho_{12\sigma} + it(\rho_{11\sigma} - \rho_{22\sigma})$$

$$- \frac{1}{2}\left[\Gamma^-_{L\sigma} + \Gamma^-_{R\sigma} + \sum_{\eta,\sigma'} \tilde{\Gamma}^+_{\eta\sigma'} \right]\rho_{12\sigma}, \tag{36d}$$

$$\dot{\rho}_{dd\sigma\sigma} = \tilde{\Gamma}^+_{R\sigma}\rho_{11\sigma} + \tilde{\Gamma}^+_{L\sigma}\rho_{22\sigma} - (\tilde{\Gamma}^-_{L\sigma} + \tilde{\Gamma}^-_{R\sigma})\rho_{dd\sigma\sigma}, \tag{36e}$$

$$\dot{\rho}_{dd\sigma\bar{\sigma}} = \tilde{\Gamma}^+_{R\bar{\sigma}}\rho_{11\sigma} + \tilde{\Gamma}^+_{L\sigma}\rho_{22\bar{\sigma}} - (\tilde{\Gamma}^-_{L\sigma} + \tilde{\Gamma}^-_{R\bar{\sigma}})\rho_{dd\sigma\bar{\sigma}}, \tag{36f}$$

and along with $\rho_{00} + \Sigma_{\sigma}(\rho_{11\sigma} + \rho_{22\sigma}) + \Sigma_{\sigma,\sigma'}\rho_{dd\sigma\sigma'} = 1$, in which $\Gamma^\pm_{\eta\sigma} = \Gamma_{\eta\sigma} f^\pm_\eta(\epsilon_d)$ and $\tilde{\Gamma}^\pm_{\eta\sigma} = \Gamma_{\eta\sigma} f^\pm_\eta(\epsilon_d + U)$ have the similar prescriptions as in the SQD. In addition, the classical parts of the diagonal elements' equations have the similar interpretations. For example, Eq. (36b) for the rate of change of the number of the spin-σ electrons in the first QD $\rho_{11\sigma}$ is contributed, noting the fact that the first (second) QD does not directly connect to the right (left) lead, from four single-particle tunneling processes: (1) tunneling into the QD with spin-σ electrons $\Gamma^+_{L\sigma}$ from the left lead if the QD is initially in the empty state ρ_{00}; (2) tunneling out from the QD with

spin-σ' electrons $\tilde{\Gamma}^-_{R\sigma'}$ into the right lead if the QD is initially in the doubly occupied state $\rho_{dd\sigma\sigma'}$; (3) tunneling into the QD with spin-σ' electrons $\tilde{\Gamma}^+_{R\sigma'}$ from the right lead; and 4) tunneling out from the QD with spin-σ electrons $\Gamma^-_{L\sigma}$ into the left lead, when the QD is initially just in this state $\rho_{11\sigma}$. Tunneling events (1) and (2) increase $\rho_{11\sigma}$, but events (3) and (4) decrease this probability. The final term in Eq. (36b) is responsible for coherent effects. Equation (36d) for the nondiagonal matrix element $\rho_{12\sigma}$ indicates that the role of the leads is to provide damping of the quantum superposition.[15] It is also worth noting that the present proposed quantum rate equations are reliable for a wide range of temperature and external bias voltage, where the three major approximations we use are valid.

The electric current I_L flowing from the lead L to the QD can be calculated as

$$I_L = ie \int \frac{d\omega}{2\pi} \sum_{\sigma} \left\{ \Gamma_{\eta\sigma} f_\eta(\omega) \left[G^>_{e11\sigma}(\omega) \right. \right.$$

$$\left. + \sum_{\sigma',\sigma''} G^>_{d22\sigma\sigma'\sigma''}(\omega) \right] + \Gamma_{\eta\sigma}[1 - f_\eta(\omega)] \left[G^<_{e11\sigma}(\omega) \right.$$

$$\left. \left. + \sum_{\sigma',\sigma''} G^<_{d22\sigma\sigma'\sigma''}(\omega) \right] \right\}. \tag{37}$$

Under the weak-coupling approximation, it becomes

$$I_L/e = \sum_{\sigma} [\tilde{\Gamma}^-_{L\sigma}(\rho_{dd\sigma\sigma} + \rho_{dd\sigma\bar{\sigma}}) + \Gamma^-_{L\sigma}\rho_{11\sigma}$$

$$- \tilde{\Gamma}^+_{L\sigma}(\rho_{22\sigma} + \rho_{22\bar{\sigma}}) - \Gamma^+_{L\sigma}\rho_{00}]. \tag{38a}$$

Similarly, for the current flowing from the lead R we have

$$I_R/e = \sum_{\sigma} [\tilde{\Gamma}^-_{R\sigma}(\rho_{dd\sigma\sigma} + \rho_{dd\bar{\sigma}\sigma}) + \Gamma^-_{R\sigma}\rho_{22\sigma}$$

$$- \tilde{\Gamma}^+_{R\sigma}(\rho_{11\sigma} + \rho_{11\bar{\sigma}}) - \Gamma^+_{R\sigma}\rho_{00}]. \tag{38b}$$

It is easy to prove that, in stationary condition, the current conservation is fulfilled $I_L = -I_R$.

C. Discussion

In order to simplify the analysis, we only consider spin-independent tunneling processes in the following discussion. Two special cases, no doubly occupied state and no empty state, are studied. First we assume the interdot Coulomb interaction U is infinite, whereas only one electron can be found inside the system, so $\rho_{dd\sigma\sigma'} = 0$ and $\tilde{\Gamma}^+_{\eta\sigma} \simeq 0$. The quantum rate equations (36b)–(36f) simplify to

$$\dot{\rho}_{11} = \Gamma^+_L \rho_{00} - \Gamma^-_L \rho_{11} - 2t\mathrm{Im}\rho_{12}, \tag{39a}$$

$$\dot{\rho}_{22} = \Gamma^+_R \rho_{00} - \Gamma^-_R \rho_{22} + 2t\mathrm{Im}\rho_{12}, \tag{39b}$$

$$\dot{\rho}_{12} = i(\epsilon_2 - \epsilon_1)\rho_{12} + it(\rho_{11} - \rho_{22}) - \frac{1}{2}(\Gamma^-_L + \Gamma^-_R)\rho_{12}, \tag{39c}$$

with $\rho_{00} + 2\rho_{11} + 2\rho_{22} = 1$. The steady solutions are

$$\rho_{11} = [\Gamma^+_L \Gamma^-_R + t^2(\Gamma^+_L + \Gamma^+_R)(\Gamma^-_L + \Gamma^-_R)/\Lambda]/\Delta, \tag{40a}$$

$$\rho_{22}=[\Gamma_L^-\Gamma_R^++t^2(\Gamma_L^++\Gamma_R^+)(\Gamma_L^-+\Gamma_R^-)/\Lambda]/\Delta, \quad (40b)$$

$$\rho_{12}=t(\Gamma_L^+\Gamma_R^--\Gamma_L^-\Gamma_R^+)[\epsilon_1-\epsilon_2+i\tfrac{1}{2}(\Gamma_L^-+\Gamma_R^-)]/\Delta\Lambda, \quad (40c)$$

$$\Delta=\Gamma_L^-\Gamma_R^-+2\Gamma_L^-\Gamma_R^++2\Gamma_L^+\Gamma_R^-+t^2(\Gamma_L^-+\Gamma_R^-+4\Gamma_L^++4\Gamma_R^+)$$

$$\times(\Gamma_L^-+\Gamma_R^-)/\Lambda, \quad (40d)$$

in which $\Lambda=(\epsilon_2-\epsilon_1)^2+(\Gamma_L^-+\Gamma_R^-)^2/4$. The steady current is given by $I_L/e=2(\Gamma_L^-\rho_{11}-\Gamma_L^+\rho_{00})$.

It is interesting to compare our results in this situation with those of Gurvitz and Prager[15] for the case of large bias voltage between the two leads. For example, the large bias voltage determines $\Gamma_L^-=0$, $\Gamma_R^+=0$ and $\Gamma_L^+=\Gamma_L$, $\Gamma_R^-=\Gamma_R$ at $eV\gg T$. Therefore, the dc current becomes

$$I_L/e=-\frac{t^2\Gamma_R}{t^2(2+\Gamma_R/2\Gamma_L)+(\Gamma_R)^2/4+(\epsilon_2-\epsilon_1)^2}, \quad (41)$$

which coincides with the result obtained by Gurvitz and Prager.[15] It is quite obvious that the finite temperature plays a crucial role in the coherence tunneling. The previous formulations for large bias voltages, however, can not provide any information about the temperature effects. This is the central improvement of the present approach for the coupled quantum systems.

Second, we consider the deep level situation where the bare levels ϵ_1 and ϵ_2 are far below the Fermi level but ϵ_d+U is just above the Fermi level in equilibrium. In this case the CQD is always occupied and $\rho_{00}=0$, $\Gamma_{\eta\sigma}^-\simeq0$. Therefore, we have

$$\dot{\rho}_{11}=2\widetilde{\Gamma}_R^-\rho_{dd}-2\widetilde{\Gamma}_R^+\rho_{11}-2t\,\mathrm{Im}\rho_{12}, \quad (42a)$$

$$\dot{\rho}_{22}=2\widetilde{\Gamma}_L^-\rho_{dd}-2\widetilde{\Gamma}_L^+\rho_{22}+2t\,\mathrm{Im}\rho_{12}, \quad (42b)$$

$$\dot{\rho}_{dd}=\widetilde{\Gamma}_R^+\rho_{11}+\widetilde{\Gamma}_L^+\rho_{22}-(\widetilde{\Gamma}_L^-+\widetilde{\Gamma}_R^-)\rho_{dd}, \quad (42c)$$

$$\dot{\rho}_{12}=i(\epsilon_2-\epsilon_1)\rho_{12}+it(\rho_{11}-\rho_{22})-(\widetilde{\Gamma}_L^++\widetilde{\Gamma}_R^+)\rho_{12}, \quad (42d)$$

with $2\rho_{11}+2\rho_{22}+4\rho_{dd}=1$. After solving the set of equations in the steady state, we obtain

$$\rho_{11}=[\widetilde{\Gamma}_L^+\widetilde{\Gamma}_R^-+t^2(\widetilde{\Gamma}_L^++\widetilde{\Gamma}_R^+)(\widetilde{\Gamma}_L^-+\widetilde{\Gamma}_R^-)/\Lambda]/\Delta, \quad (43a)$$

$$\rho_{22}=[\widetilde{\Gamma}_L^-\widetilde{\Gamma}_R^++t^2(\widetilde{\Gamma}_L^++\widetilde{\Gamma}_R^+)(\widetilde{\Gamma}_L^-+\widetilde{\Gamma}_R^-)/\Lambda]/\Delta, \quad (43b)$$

$$\rho_{12}=t(\widetilde{\Gamma}_L^+\widetilde{\Gamma}_R^--\widetilde{\Gamma}_L^-\widetilde{\Gamma}_R^+)[\epsilon_1-\epsilon_2+i(\widetilde{\Gamma}_L^++\widetilde{\Gamma}_R^+)]/\Delta\Lambda, \quad (43c)$$

$$\Delta=2\widetilde{\Gamma}_L^+\widetilde{\Gamma}_R^-+2\widetilde{\Gamma}_L^-\widetilde{\Gamma}_R^++4\widetilde{\Gamma}_L^+\widetilde{\Gamma}_R^++4t^2(\widetilde{\Gamma}_L^-+\widetilde{\Gamma}_R^-+\widetilde{\Gamma}_L^++\widetilde{\Gamma}_R^+)$$

$$\times(\widetilde{\Gamma}_L^++\widetilde{\Gamma}_R^+)/\Lambda, \quad (43d)$$

in which $\Lambda=(\epsilon_2-\epsilon_1)^2+(\widetilde{\Gamma}_L^++\widetilde{\Gamma}_R^+)^2$. The dc current is $I_L/e=4(\widetilde{\Gamma}_L^-\rho_{dd}-\widetilde{\Gamma}_L^+\rho_{22})$.

It is also interesting to consider the situation of large bias voltage in the strong interdot Coulomb repulsion U, whereas
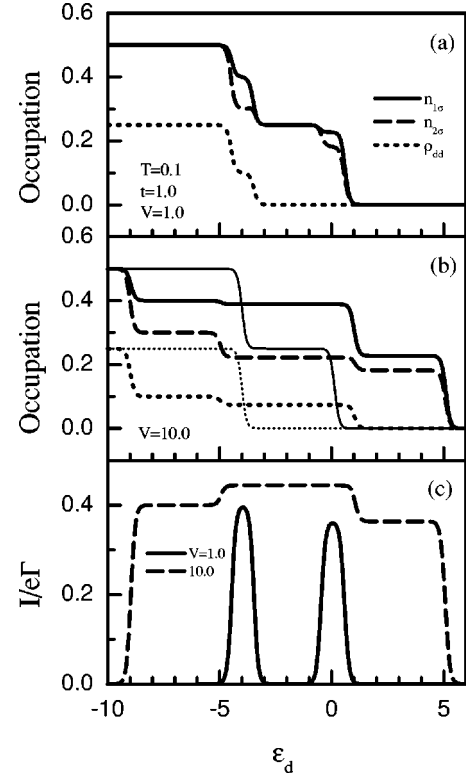

FIG. 5. Nonequilibrium occupation numbers $n_{1\sigma}$, $n_{2\sigma}$, ρ_{dd} (a,b), and current (c) vs the bare level of the CQD. (a) is plotted at a small bias $V=1.0$ and (b) is at a large bias $V=10.0$. The equilibrium occupation numbers are also depicted by the thin lines in (b) and (e). Other parameters are $U=4$, $T=0.1$, and $t=1.0$.
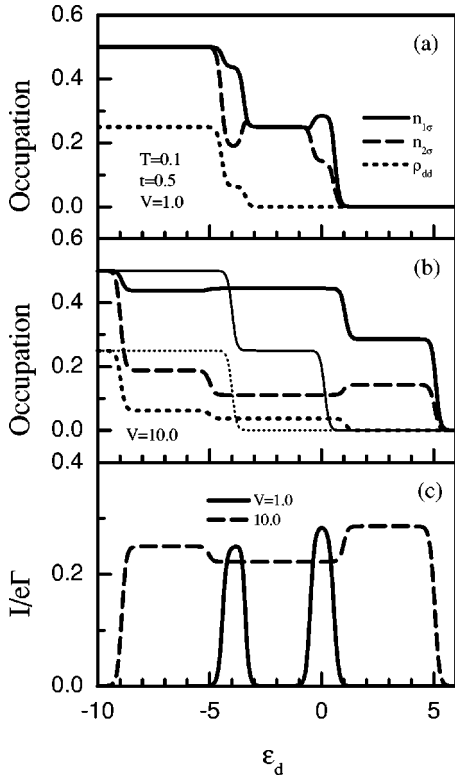
the Fermi level of the right lead μ_R lies far below ϵ_d+U, but far above the resonance level ϵ_d to satisfy the requirement of deep level, meanwhile the Fermi level of the left lead μ_L is far above ϵ_d+U, so that $\widetilde{\Gamma}_L^-=0$, $\widetilde{\Gamma}_R^+=0$ and $\widetilde{\Gamma}_L^+=\Gamma_L$, $\widetilde{\Gamma}_R^-=\Gamma_R$. Finally we obtain

$$I_L/e=-\frac{2t^2\widetilde{\Gamma}_L}{2t^2(1+\widetilde{\Gamma}_L/\widetilde{\Gamma}_R)+2(\epsilon_2-\epsilon_1)^2+(\widetilde{\Gamma}_L)^2}. \quad (44)$$

D. Numerical results

In this section, we perform numerical calculations for the tunneling transport through the CQD, by using the quantum rate equations (36), in the stationary condition. We symmetrically add the bias voltage again between the source and drain $\mu_L=-\mu_R=eV/2$.

First we consider the spin-independent transport. Figure 5 demonstrates the nonequilibrium occupation numbers in the first and the second QD's, calculated from the obtained expectation values of density-matrix elements $n_{1\sigma}=\rho_{11\sigma}+\Sigma_{\sigma'}\rho_{dd\sigma\sigma'}$ and $n_{2\sigma}=\rho_{22\sigma}+\Sigma_{\sigma'}\rho_{dd\sigma'\sigma}$, and the corresponding current versus the discrete level for the hopping $t=1.0$ between the two QD's at a small bias $V=1.0$ and a large bias $V=10.0$, respectively. We find a similar characteristic as in the SQD (Fig. 2): (1) The nonzero bias weakens the Coulomb blockade effect; (2) $n_{1\sigma}$ and $n_{2\sigma}$ have fractional steps; (3) $n_{1\sigma}\neq n_{2\sigma}$ in nonequilibrium; (4) and the

FIG. 6. Same as Fig. 5 except for $t=0.5$.

FIG. 7. Occupation numbers $n_{1\sigma}$, $n_{2\sigma}$, ρ_{dd} (a,d), current (b,e), and the differential conductance (c,f) vs the bias voltage, calculated for different hopping t. (a)–(c) are plotted for $\epsilon_d=1$, (d)–(f) for $\epsilon_d=-5$. Other parameters are as in Fig. 5.

conductance has two peaks at the resonant points, while the current has three steps in the strong nonequilibrium regime. Here we observe a higher peak magnitude and a higher step value at the deep level regime than those at the no doubly occupied level regime, and the maximum step value located at the middle "window" of the bare level. More interestingly, an opposite behavior has been found when the hopping t between two QD's decreases, as shown in Fig. 6(c), in which we plot the corresponding results for a small hopping $t=0.5$. Generally, one may expect that increasing the hopping t can reduce the difference between two QD's, and very strong hopping can finally give rise to the formation of covalence. In other words, the difference between $n_{1\sigma}$ and $n_{2\sigma}$ should rise with decreasing the hopping t. This is the case as shown in Figs. 6(a) and 6(b), where the occupation numbers are displayed for the smaller hopping $t=0.5$ in comparison with the results of the hopping $t=1.0$ in Figs. 5(a) and 5(b). One can note that the occupation number in the second QD even experiences a descendance in the middle "window" of the bare level for the case of $t=0.5$, which expresses an opposite behavior in the case of $t=1.0$. This is the reason why current-voltage characteristics are different in the two cases.

The effect of the hopping on the tunneling is more clearly illustrated in Fig. 7, where we plot the occupation numbers, the current, and the differential conductance as a function of the bias for different hoppings t in the no doubly occupied level $\epsilon_d=1$ and the deep level $\epsilon_d=-5$. In both cases, we have two peaks in the differential conductance corresponding to the two steps in the current. More importantly, we find that the current declines in the second step and consequently the
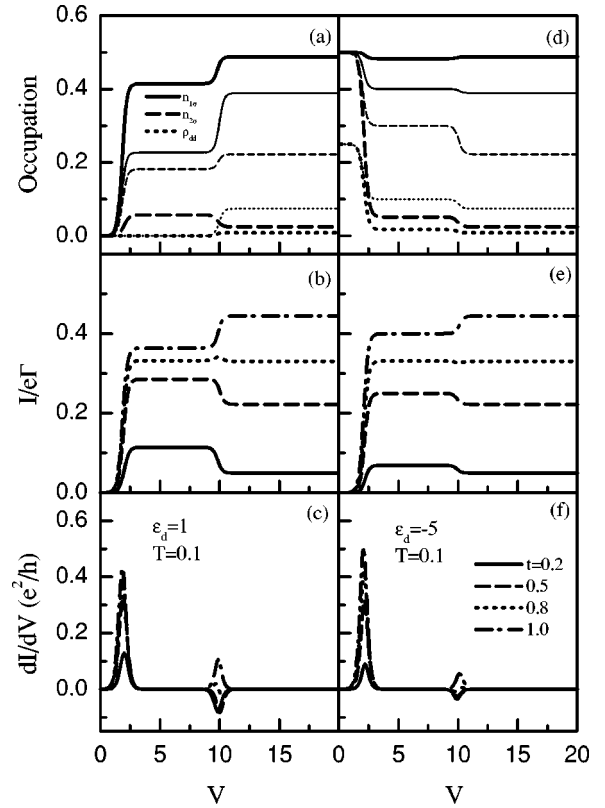
negative differential conductance (NDC) appears in the according biases when the hopping $t<1.0$. We can explain the appearance of the NDC by variations of the occupation numbers with the bias, as shown in Figs. 7(a) and 7(d) for the hoppings $t=0.2$ (thick lines) and $t=1.0$ (thin lines). Considering the fact that we apply the bias symmetrically and $\mu_R=-eV/2<0$, the current flowing from the right lead is dominated for the case $\epsilon_d=1$ by the process: tunneling out from the second QD into the right lead. According to Eq. (38b), we have $I_R/e\approx\Sigma_\sigma\Gamma_{R\sigma}n_{2\sigma}$. It is obvious from Fig. 7(a) that the rising second step in $n_{2\sigma}$ for the case of $t=1.0$ (thin dashed curve) indicates the rising step in the current, whereas the declining second step for the case of $t=0.2$ (thick dashed curve) implies the NDC. In the other case $\epsilon_d=-5$, the current flowing from the left lead is ruled by the tunneling process into the first QD from the left lead, being approximately $I_L/e\approx\Sigma_\sigma\Gamma_{L\sigma}[1-n_{1\uparrow}-n_{1\downarrow}]$. Apparently, the variations of $n_{1\sigma}$ denoted by the solid lines in Fig. 7(d) provide interpretations for the current-voltage characteristic in Fig. 7(e) and the NDC in Fig. 7(f). Therefore, it can be addressed that opening of a new channel provides negative contribution to the current in the case of $t\lesssim1.0$.

An interesting question is what happens to the tunneling current and the NDC when the interdot Coulomb interaction U weakens or strengthens. We show this in Fig. 8, where current vs bias is presented for various correlation parameters from $U=0$ to ∞ in the cases $t=1.0$ (thick lines) and
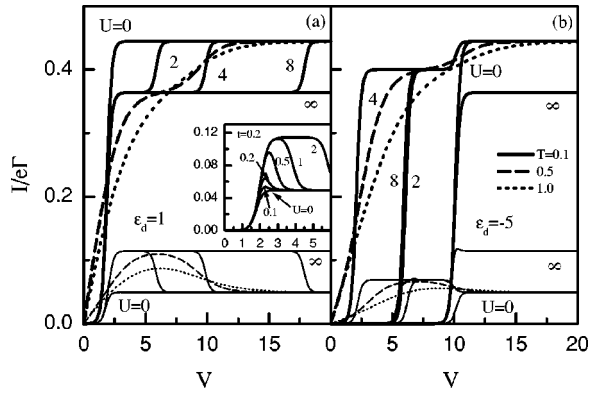
FIG. 8. The current-voltage characteristics, calculated for indicated values of the interdot Coulomb interaction U and different hoppings $t=0.2$ (thin lines) and 1.0 (thick lines). (a) is plotted for $\epsilon_d=1$ and (b) is for $\epsilon_d=-5$. Inset in (a): I-V curves for small U.

$t=0.2$ (thin lines). For $U\rightarrow\infty$, the current has only one step with increasing bias in both cases of $\epsilon_d=1$ (a) and $\epsilon_d=-5(b)$, because no new channel is available due to the extremely strong charging effect. For the finite interdot Coulomb correlation, however, the applied bias can overcome the Coulomb blockade effect and open a new channel for tunneling at the corresponding threshold value of voltage. For $t\lesssim1.0$, this new channel induces a peak in the current. This peak becomes narrower with declining value of U, but its height remains unchanged if U is not too small. At sufficiently small values of U, as shown in the inset of Fig. 8(a), height of the peak in current decreases, even vanishes finally when $U=0$. So we can claim that the interdot Coulomb interaction $U=0$ and ∞ leads to the single peak in the differential conductance, but the finite values result in double peaks, and even the NDC in the case of $t\lesssim1.0$.

The temperature effect is also shown in Fig. 8 for $U=4$. Increasing temperature smoothes I-V curve, but remains the NDC unchanged.

Now we study the spin-dependent tunneling through the CQD connected to two ferromagnetic leads. Figures. 9 and 10 depict the occupation numbers in the two QD's and the current in both P and AP configurations for $\epsilon_d=1$ and $\epsilon_d=-5$, respectively. We find, besides analogous behaviors with the spin-independent tunneling, that (1) $n_{1\uparrow}\neq n_{1\downarrow}$ even in both alignments; (2) $n_{2\uparrow}\simeq n_{2\downarrow}$ in the P configuration but $n_{2\uparrow}\neq n_{2\downarrow}$ in the AP configuration; (3) variations of the current flowing in different magnetic configurations are very sensitive to the value of the hopping between two QD's, which leads to (4) the negative TMR for the sufficiently small hopping $t=0.2$, as exhibited in Figs. 9(c) and 10(c) at certain voltages.

IV. CONCLUSION

In this paper, we have systematically derived the quantum rate equations for sequential tunneling from NGF, and then utilized them to investigate quantum coherent transport in a single QD with weak spin-flip scattering and weakly coupled QD's systems taking the intradot and interdot Coulomb interactions into account. In these systems, the superposition

between different states plays a vitally important role in coherent tunneling processes. Directly, a kind of quantum oscillations in mesoscopic systems is due to this superposition effect. Now, it is believed that the master equations or the modified quantum rate equations, which are actually equations of motion of density submatrix for diagonal and nondiagonal elements, provide a successful tool to study this phenomenon, and even allow an analytical description.

For this purpose, we have generalized the slave-particle technique, which was developed previously in the single-site space and successfully applied to study the strongly correlated systems, into the two-site space. Based on this theoretical approach and the correct quantization of these artificially introduced operators, previously well-developed NGF for noninteracting systems has been used to construct the quantum rate equations when only three assumptions are made: first, the coupling between the central region and the leads
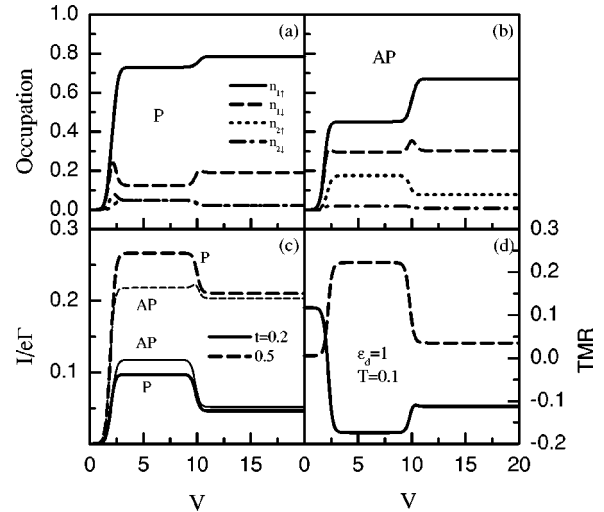

FIG. 9. Occupation numbers $n_{1\uparrow}$, $n_{1\downarrow}$, $n_{2\uparrow}$, and $n_{2\downarrow}$ in the P configuration (a) and the AP configuration (b) for $t=0.2$, current (c), and TMR (d) for $t=0.2$ and 0.5 vs the bias voltage. Other parameters are $\epsilon_d=1$, $T=0.1$, and $p=0.5$.
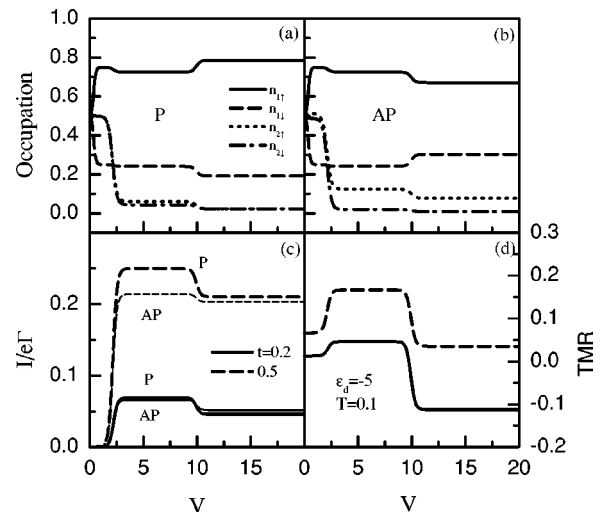

FIG. 10. Same as Fig. 9 but for the case of $\epsilon_d=-5$.

must be weak; second, the couplings between the subsystems are also weak, for example, weak spin-flip scattering in SQD and weak interdot hopping in CQD; and third, the wide band limit. The first condition makes it valid that we can keep only the lowest order terms in $|V|^2$ in the expansion of the equations of motion. It also renders the central region approximately a quasiequilibrium isolated system, which facilitates the "localized" energy spectrum expressions for the correlation GF's of every subsystem in the central region in combination with the second presumption. These approximations notwithstanding our approach is appropriate for a wide range of temperature and external bias voltage, and incorporation of the charging effect. Finally, it should be pointed out that our derivation is equivalent to the lowest-order gradient expansion technique.[25]

Employing this approach, we have studied in detail the coherent tunneling through a SQD and a CQD system. We have given some analytic expressions for steady-state transport in two special cases: doubly occupied prohibited state and deep level in large intradot or interdot Coulomb repulsion. Furthermore, we have compared some of our results with previously obtained results in the literature. For example, for resonant tunneling through a SQD with spin-flip scattering, our approach provides a quantum correction to the classical results. When there is no spin-flip scattering, our rate equations reduce exactly to the classical results as Glazman and Matveev,[33] and Beenakker.[34] In the case of resonant tunneling through a CQD, our results are in perfect agreement with the previous analysis proposed by Gurvitz and Prager[15] under the limitation of zero temperature and large bias voltage.

In addition, we have performed numerical simulations for variations of occupation numbers and the current with increasing the bias voltage and varying the discrete level in QD. We summarize the main common features as follows: (1) Occupation numbers have fractional steps in nonequilibrium, implying that the Coulomb blockade effect is partially overcome by applying bias voltage, and correspondingly (2) the current-voltage characteristic displays two steps, giving rise to double peaks in the differential conductance. Especially, our calculations manifest the importance of temperature and bias on the spin-flip transitions in the SQD. For the CQD, a possible NDC can be reached if the interdot Coulomb interaction is finite and the hopping between two QD's is small $t \lesssim 1.0$. Besides, the TMR becomes negative in nonequilibrium for the CQD connected to two ferromagnetic leads if the hopping t is sufficiently small.

**APPENDIX DERIVATION OF QUANTUM RATE
EQUATIONS FOR SQD**

In the appendix, we present a detailed derivation of Eqs. (11). In the following, we take Eq. (11b) as an example. The statistical expectation of Eq. (10b) gives

$$\rho_{\sigma\sigma} = \sum_{\eta,k} [V_{\eta\sigma}G^<_{e\sigma,\eta k\sigma}(t,t) - \bar{\sigma}V_{\eta\bar{\sigma}}G^<_{d\sigma,\eta k\bar{\sigma}}(t,t)$$
$$- V^*_{\eta\sigma}G^<_{\eta k\sigma,e\sigma}(t,t) + \bar{\sigma}V^*_{\eta\bar{\sigma}}G^<_{\eta k\bar{\sigma},d\sigma}(t,t)]$$
$$+ iR^*_\sigma\rho_{\sigma\bar{\sigma}} - iR_\sigma\rho_{\bar{\sigma}\sigma}. \tag{A1}$$

According to Langreth's operational rules,[31] those hybrid correlation GF's are given by

$$G^<_{e\sigma,\eta k\sigma'}(t,t') = \delta_{\sigma\sigma'}\int dt_1[G^r_{e\sigma\sigma}(t,t_1)V^*_{\eta\sigma'}g^<_{\eta k\sigma'}(t_1,t')$$
$$+ G^<_{e\sigma\sigma}(t,t_1)V^*_{\eta\sigma'}g^a_{\eta k\sigma'}(t_1,t')], \tag{A2a}$$

$$G^<_{d\sigma,\eta k\sigma'}(t,t') = \delta_{\sigma\bar{\sigma}'}\sigma'\int dt_1[G^r_{d\sigma\sigma}(t,t_1)V^*_{\eta\sigma'}g^<_{\eta k\sigma'}(t_1,t')$$
$$+ G^<_{d\sigma\sigma}(t,t_1)V^*_{\eta\sigma'}g^a_{\eta k\sigma'}(t_1,t')], \tag{A2b}$$

$$G^<_{\eta k\sigma',e\sigma}(t,t') = \delta_{\sigma\sigma'}\int dt_1[g^r_{\eta k\sigma'}(t,t_1)V_{\eta\sigma'}G^<_{e\sigma\sigma}(t_1,t')$$
$$+ g^<_{\eta k\sigma'}(t,t')V_{\eta\sigma'}G^a_{e\sigma\sigma}(t_1,t')], \tag{A2c}$$

$$G^<_{\eta k\sigma',d\sigma}(t,t') = \delta_{\sigma\bar{\sigma}'}\sigma'\int dt_1[g^r_{\eta k\sigma'}(t,t_1)V_{\eta\sigma'}G^<_{d\sigma\sigma}(t_1,t')$$
$$+ g^<_{\eta k\sigma'}(t,t')V_{\eta\sigma'}G^a_{d\sigma\sigma}(t_1,t')]. \tag{A2d}$$

Substituting Eqs. (A2) into Eq. (A1) and taking the Fourier transformation, $\rho_{\sigma\sigma}$ can be expressed as

$$\rho_{\sigma\sigma} = \frac{1}{2\pi}\int d\omega \sum_{\eta,k} |V_{\eta\sigma}|^2\{[G^r_{e\sigma\sigma}(\omega) - G^a_{e\sigma\sigma}(\omega)]g^<_{\eta k\sigma}(\omega)$$
$$+ G^<_{e\sigma\sigma}(\omega)[g^a_{\eta k\sigma}(\omega) - g^r_{\eta k\sigma}(\omega)]\} + |V_{\eta\bar{\sigma}}|^2\{[G^a_{d\sigma\sigma}(\omega)$$
$$- G^r_{d\sigma\sigma}(\omega)]g^<_{\eta k\bar{\sigma}}(\omega) + G^<_{d\sigma\sigma}(\omega)(g^r_{\eta k\bar{\sigma}}(\omega) - g^a_{\eta k\bar{\sigma}}(\omega))]\}$$
$$+ iR^*_\sigma\rho_{\sigma\bar{\sigma}} - iR_\sigma\rho_{\bar{\sigma}\sigma}, \tag{A3}$$

where $g_{\eta k\sigma}(\omega)$ are the Fourier transform of the exact GF's in the ηth lead without the coupling to the central region. In the wide band limit, one has

$$\sum_k |V_{\eta\sigma}|^2 g^<_{\eta k\sigma}(\omega) = i\Gamma_{\eta\sigma}f_\eta(\omega), \tag{A4a}$$

$$\sum_k |V_{\eta\sigma}|^2 g^>_{\eta k\sigma}(\omega) = -i\Gamma_{\eta\sigma}[1 - f_\eta(\omega)]. \tag{A4b}$$

Substituting the GF's (A4) into Eq. (A3) and employing $G^r - G^a \equiv G^> - G^<$, Eq. (11b) can be reached. Analogously, we can derive other equations in Eq. (11).

[1] D.V. Averin and K.K. Likharev, in *Mesoscopic Phenomena in Solids*, edited by B. Altshuler, P.A. Lee, and R.A. Webb (Elsevier, Amsterdam, 1991).

[2] T.K. Ng and P.A. Lee, Phys. Rev. Lett. **61**, 1768 (1988).

[3] L. Kouwenhoven and L. Glazman, Phys. World **14**, 33 (2001).

[4] N.C. van der Vaart, S.F. Godijn, Y.V. Nazarov, C.J.P.M. Harmans, J.E. Mooij, L.W. Molenkamp, and C.T. Foxon, Phys. Rev. Lett. **74**, 4702 (1995); F.R. Waugh, M.J. Berry, D.J. Mar, R.M. Westervelt, K.L. Campman, and A.C. Gossard, *ibid.* **75**, 705 (1995).

[5] R.H. Blick, D. Pfannkuche, R.J. Haug, K. v. Klitzing, and K. Eberl, Phys. Rev. Lett. **80**, 4032 (1998).

[6] T.H. Oosterkamp, T. Fujisawa, W.G. vander Wiel, K. Ishibashi, R.V. Hijman, S. Tarucha, and L.P. Kouwenhoven, Nature (London) **395**, 873 (1998).

[7] For a review, see W.G. van der Wiel, S. De Franceschi, J.M. Elzerman, T. Fujisawa, S. Tarucha, and L.P. Kouwenhoven, Rev. Mod. Phys. **75**, 1 (2003).

[8] G. Prinz, Science **282**, 1660 (1998); S.A. Wolf *et al.*, *ibid.* **294**, 1488 (2001).

[9] Y. Manassen, I. Mukhopadhyay, and N. Ramesh Rao, Phys. Rev. B **61**, 16223 (2000); Y. Manassen, R.J. Hamers, J.E. Demuth, and A.T. Castellano, Jr., Phys. Rev. Lett. **62**, 2531 (1989); C. Durkan and M.E. Welland, Appl. Phys. Lett. **80**, 458 (2002).

[10] A.V. Balatsky and I. Martin, cond-mat/0112407; D. Mozyrsky, L. Fedichkin, S.A. Gurvitz, and G.P. Berman, Phys. Rev. B **66**, 161313 (2002); Jian-Xin Zhu and A.V. Balatsky, Phys. Rev. Lett. **89**, 286802 (2002).

[11] M.H. Hettler, H. Schoeller, and W. Wenzel, Europhys. Lett. **57**, 571 (2002); P. Hyldgaard, and B.I. Lundqvist, Solid State Commun. **116**, 569 (2000).

[12] M.H. Hettler, W. Wenzel, M.R. Wegewijs, and H. Schoeller, Phys. Rev. Lett. **90**, 076805 (2003).

[13] D. Porath, A. Bezryadin, S. de Vries, and C. Dekker, Nature (London) **403**, 635 (2000).

[14] Yu.V. Nazarov, Physica B **189**, 57 (1993).

[15] S.A. Gurvitz and Ya.S. Prager, Phys. Rev. B **53**, 15 932 (1996).

[16] S.A. Gurvitz, Phys. Rev. B **57**, 6602 (1998).

[17] H.-A. Engel and D. Loss, Phys. Rev. Lett. **86**, 4648 (2001); Phys. Rev. B **65**, 195321 (2002).

[18] A.N. Korotkov, Phys. Rev. B **60**, 5737 (1999); **63**, 115403 (2001); **67**, 075303 (2003).

[19] H.-S. Goan, G.J. Milburn, H.M. Wisernan, and H.B. Sun, Phys. Rev. B **63**, 125326 (2001).

[20] B. Elattari and S.A. Gurvitz, Phys. Rev. Lett. **84**, 2047 (2000); Phys. Rev. A **62**, 032102 (2000).

[21] T.H. Stoof and Yu.V. Nazarov, Phys. Rev. B **55**, 1050 (1999); B.L. Hazelzet, M.R. Wegewijs, T.H. Stoof, and Yu.V. Nazarov, *ibid.* **63**, 165313 (2001).

[22] C.A. Stafford and N.S. Wingreen, Phys. Rev. Lett. **76**, 1916 (1996).

[23] S.A. Gurvitz, Phys. Rev. B **56**, 15215 (1997); S.A. Gurvitz, quant-ph/9607029; quant-ph/9808058; quant-ph/0303177.

[24] M. Büttiker and A.M. Martin, Phys. Rev. B **61**, 2737 (2000); M. Büttiker, Lect. Notes Phys. **579**, 149 (2001).

[25] J.H. Davies, S. Hershfield, P. Hyldgaard, and J.W. Wilkins, Phys. Rev. B **47**, 4603 (1993).

[26] Ned S. Wingreen, and Y. Meir, Phys. Rev. B **49**, 11040 (1994); M.H. Hettler, J. Kroha, and S. Hershfield, *ibid.* **88**, 5649 (1998).

[27] R. Aguado and D.C. Langreth, Phys. Rev. Lett **85**, 1946 (2000); B. Dong and X.L. Lei, Phys. Rev. B **63**, 235306 (2001); B. Dong and X.L. Lei, J. Phys.: Condens. Matter **13**, 9245 (2001).

[28] A. C. Hewson, *The Kondo Problem to Heavy Fermions* (Cambridge University Press, Cambridge, 1993).

[29] Z. Zou and P.W. Anderson, Phys. Rev. B **37**, 627 (1988).

[30] J.C. Le Guillou and E. Ragoucy, Phys. Rev. B **52**, 2403 (1995).

[31] D. C. Langreth, in *Linear and Nonlinear Electron Transport in Solids*, Vol. 17 of *Nato Advanced Study Institute, Series B: Physics*, edited by J. T. Devreese and V. E. Van Doren (Plenum, New York, 1976).

[32] Y. Meir and N.S. Wingreen, Phys. Rev. Lett. **68**, 2512 (1992).

[33] L.I. Glazman and K.A. Matveev, Pis'ma Zh. Éksp. Teor. Fiz. **48**, 403 (1988) [JETP Lett. **48**, 445 (1988)].

[34] C.W.J. Beenakker, Phys. Rev. B **44**, 1646 (1991).

[35] W. Rudziński and J. Barnaś, Phys. Rev. B **64**, 085318 (2001).